

Rapid granular flows down inclined planar chutes. Part 1. Steady flows, multiple solutions and existence domains

MARK J. WOODHOUSE†, ANDREW J. HOGG
AND ALISTAIR A. SELLAR

Department of Mathematics, University of Bristol, University Walk, Bristol BS8 1TW, UK

(Received 28 May 2009; revised 14 January 2010; accepted 15 January 2010)

The highly agitated flow of grains down an inclined chute is modelled using a kinetic theory for inelastic collisions. Solutions corresponding to steady, fully developed flows are obtained by solving numerically a nonlinear system of ordinary differential equations using a highly accurate pseudospectral method based on mapped Chebyshev polynomials. The solutions are characterized by introducing macroscopic, depth-integrated variables representing the mass flux of flowing material per unit width, its centre-of-mass and the mass supported within the flowing layer, and the influence of the controlling parameters on these solutions is investigated. It is shown that, in certain regions of parameter space, multiple steady solutions can be found for a specified mass flux of material. An asymptotic analysis of the governing equations, appropriate to highly agitated flows, is also developed and these results aid in the demarcation of domains in parameter space where steady solutions can be obtained.

1. Introduction

Gravity-driven flows of granular material occur extensively in industrial and environmental settings and there are pressing needs to develop predictive models of their motion. In industry, manufacturing processes involving grains often operate below the design performance: an accurate physical description of granular flows would aid in the design and operation of grain handling processes. In nature, the familiar examples of snow avalanches, rockfalls and pyroclastic flows can have a devastating effect on human life. As population pressure continues to increase habitation in areas at risk from these flows, accurate modelling is required to mitigate their impact. However, the understanding of granular media remains incomplete and there is currently no continuum model capable of describing granular flow across the observed regimes (Jaeger, Nagel & Behringer 1996; Forterre & Pouliquen 2008).

When the granular assembly is highly agitated the grains interact predominantly through instantaneous collisions. An analogy can be made between the uncorrelated grain motion and the motion of molecules in a gas. By drawing on this analogy and adapting the kinetic theory of dense gases (Chapman & Cowling 1970) to inelastic collisions, granular kinetic theories have been developed to describe the bulk flow in this

† Present address: School of Mathematics, Alan Turing Building, University of Manchester, Oxford Road, Manchester M13 9PL, UK.
Email address for correspondence: mark.woodhouse@manchester.ac.uk

collisional regime (Jenkins & Savage 1983; Lun *et al.* 1984; Jenkins & Richman 1985; Campbell 1990; Sela & Goldhirsch 1998; Garzó & Dufty 1999; Goldhirsch 2003).

The kinetic theory description introduces the ‘granular temperature’ as the kinetic energy associated with fluctuations, and it is a measure of the energy content of the flow (Campbell 1990). Since energy is lost in inelastic collisions, in the absence of a supply of energy, the granular temperature rapidly falls and the grains form high-density clusters with enduring particle contacts (McNamara & Young 1992, 1994). In order to maintain the collisional flow it is therefore necessary to supply energy to the grain assembly. In a shearing flow of grains, fluctuation energy is produced by shear work and transported by the motion of grains, as well as through particle collisions. A balance of production, conduction and dissipation of granular temperature can prevent inelastic collapse and allows a rapid flow to persist.

Inclined planar chutes present a simple geometry for laboratory experiments (examples include Savage 1979; Ahn, Brennen & Sabersky 1991; Drake 1991; Azanza, Chevoir & Moucheront 1999; Forterre & Pouliquen 2001), which have been performed extensively to guide the development of continuum models and to assess the predictions of these models (see e.g. Johnson, Nott & Jackson 1990; Richman & Marciniec 1990; Ahn, Brennen & Sabersky 1992; Anderson & Jackson 1992; Forterre & Pouliquen 2002; Mitarai & Nakanishi 2004). These studies demonstrate the rich character of solutions corresponding to steady, fully developed flows. Here, in Part 1, we calculate the steady profiles of velocity, granular temperature and volume fraction and investigate the influence of the controlling parameters on the solutions for the flow. Through our development of a Chebyshev pseudospectral method, which we couple to a parametric continuation algorithm, we can calculate steady solutions to high accuracy and with efficiency, and vary the controlling parameters to elucidate the domains in parameter space where steady solutions exist, and the character of these solutions. Interestingly, we find that, in some regions of parameter space, multiple solutions exist for a fixed mass flux of material. For some parameter values, it is possible to have three solutions for a specified mass flux; for others, there is a minimum mass flux for which solutions can be obtained and above this minimum there are always two solutions for a specified mass flux, whereas in some regions of parameter space only a single solution is possible. Furthermore, we demonstrate the robustness of the steady solutions to changes in the continuum model, in particular, assessing the influence of the form of the boundary conditions employed to model the free surface of the flow.

Comparisons between existing experiments and solutions of the kinetic theory continuum model are inevitably limited by the measurement of quantities at sidewalls rather than interior measurements of the velocity, density, pressure and stress fields. We therefore characterize our solutions by macroscopic, depth-integrated variables and focus particular attention on the relationship between the flow depth and the imposed flux of material, finding multiple solutions for a fixed mass flux of material.

Recent theoretical studies of granular chute flows have been focused on the dense flow regime (Jenkins 2006, 2007; Kumaran 2008) with the aim of enhancing the basic kinetic theory to provide a continuum model capable of describing the features of dense granular flows elucidated by discrete element modelling (Silbert *et al.* 2001, 2002, 2007; Mitarai & Nakanishi 2005). These extensions are appropriate for dense flows, indeed Jenkins (2007) alters the basic kinetic theory only when the volume fraction of grains $\nu > 0.49$. At concentrations below this value, Jenkins (2007) applies the constitutive relations from the basic kinetic theory where this simple theory is thought to be adequate to describe rapid granular flows. We limit our study to these

relatively dilute flows, and employ the constitutive relations provided by the basic kinetic theory of Lun *et al.* (1984) and Jenkins & Richman (1985), which have been shown to reproduce many of the features of rapid granular flows seen in experiments (Ahn *et al.* 1991; Azanza *et al.* 1999; Hanes & Walton 2000) and discrete element simulations (such as Campbell & Brennen 1985; Walton 1993; Zheng & Hill 1996; Hanes & Walton 2000). We anticipate that the methodology we develop in this study could be readily applied to the more elaborate models for dense granular flows.

This paper is organized as follows. In §2 the continuum model, derived from a granular kinetic theory, is presented. Solutions corresponding to steady, fully developed flows are obtained numerically in §3 through the development of a mapped Chebyshev pseudospectral method. We focus particular attention on the characterization of the solutions through macroscopic, depth-integrated variables, in particular, investigating the relationship between the mass flux of material and the centre-of-mass of the flow. While the majority of our analysis is performed with asymptotic free surface conditions, in §3.7 we employ the surface boundary conditions of Jenkins & Hanes (1993) which enforce conditions at an interface between the collisional flow and saltating grains and show that our results are robust to this change. We also show in the Appendix that the modified Fourier form of the heat flux has little influence for the inclined chute flows. Steady solutions can be found only in certain regions of parameter space and in §4 we predict the existence domains with the aid of an asymptotic analysis of the governing equations, appropriate for high temperature, dilute flows. A summary of our results is given in §5.

In Woodhouse & Hogg (2010, subsequently referred to as Part 2) we go on to assess the linear stability of the steady solutions to small perturbations in three dimensions, extending the analysis of Forterre & Pouliquen (2002) and Mitarai & Nakanishi (2004). Here the highly accurate polynomial approximation of the steady solutions, which we obtain via the Chebyshev pseudospectral approach, greatly aids the linear stability analysis. Our analysis shows the existence of a continuous spectrum of eigenvalues which appears among the discrete normal mode eigenvalues and which leads to the requirement of high accuracy in the numerical approximation of the steady solutions and the perturbations. We demonstrate the existence of three qualitatively different forms for the unstable perturbations, and investigate the linear stability of steady solutions as the controlling parameters are varied, with a particular focus on the linear stability along macroscopic flow curves.

2. Kinetic theory continuum model of granular flows

In this section we briefly present the kinetic theory continuum model of Lun *et al.* (1984) (derived independently by Jenkins & Richman 1985) which we adopt in this study to describe the highly agitated flow of grains down an inclined planar chute. Granular kinetic theory has been extended to include the effects of particle roughness, either phenomenologically (Johnson & Jackson 1987) or by including friction in the micromechanical description (Jenkins & Zhang 2002), and more recently to incorporate the emergence of particle chains and clusters (Jenkins 2006, 2007). While it is possible that these extensions will enhance the agreement with experiments, the simple theory has been applied more widely (e.g. in the recent studies of Forterre & Pouliquen 2002 and Mitarai & Nakanishi 2004) and appears capable of describing many of the key features of rapid granular flows. However, the rich parameter space remains poorly investigated. For example, Ahn *et al.* (1992) employ a kinetic theory continuum model to describe steady, fully developed flows down inclined chutes

and classify their solutions into three types: flows which are productive throughout the interior, flows which are dissipative throughout the interior and flows which have productive regions and dissipative regions. However, it is not clear how these solutions are controlled by the material parameters and, in addition, Ahn *et al.* (1992) employ base boundary conditions which fix the mean field variables at the base rather than enforcing the physical mass, momentum and energy flux conditions we adopt here. Productive and dissipative flows have also been found by Anderson & Jackson (1992) and by determining solutions analytically for simplified constitutive relationships, in the regime of high density, the character of solutions can be elucidated as the controlling parameters are varied. In §4 we determine the existence of solutions as the governing parameters are varied. To this end we show that it is useful to analyse dilute highly agitated flows, and we determine asymptotic representations of the granular temperature, velocity and volume fraction of particles in this regime. Our analysis provides a method of determining whether a given set of controlling parameters results in productive or dissipative flows, and yields results that share some features with that of Anderson & Jackson (1992).

The chute flow study of Richman & Marciniec (1990), in which an approximate analytical solution of a kinetic theory continuum model is developed, demonstrates the existence of two steady flow solutions for a fixed mass flux of material, one a dilute, fast and deep flow and the other dense, slow, and shallow. Multiple solutions have been observed in the chute flow experiments of Johnson *et al.* (1990) and obtained in kinetic continuum models (Johnson *et al.* 1990; Anderson & Jackson 1992; Nott & Jackson 1992). The theory of Johnson *et al.* (1990) includes a phenomenological extension of the kinetic theory to account for frictional interactions between grains, and Anderson & Jackson (1992) compare this model with a purely collisional kinetic continuum description. Anderson & Jackson (1992) suggest the collisional theory predicts a maximum flow rate at which steady solutions are possible, which is not observed in experiment (Johnson *et al.* 1990; Hanes & Walton 2000). When using the frictional extension to the collisional theory, Anderson & Jackson (1992) show the maximum flow rate is no longer predicted and suggest that the frictional contribution is necessary to obtain solutions with the behaviour observed in experiments. This is in contrast to the results we obtain, where no maximum flow rate is predicted by our purely collisional continuum description.

2.1. Governing equations

We model a rapid granular flow as a continuum, with ‘hydrodynamic’ equations describing the evolution of the mean field variables. These mean field variables are the density ρ , the mean velocity $\mathbf{u} = (u, v, w)$ and the granular temperature $T = \langle C^2 \rangle / 3$ where \mathbf{C} represents the fluctuation velocity of grains away from the mean velocity and $\langle \dots \rangle$ denotes an average over microscopic (grain-scale) configurations. The continuum equations governing the time evolution and spatial variations of the mean field variables under a gravitational body force are

$$\frac{D\rho}{Dt} = -\rho \nabla \cdot \mathbf{u}, \quad (2.1)$$

$$\rho \frac{D\mathbf{u}}{Dt} = \rho \mathbf{g} - \nabla \cdot \mathbf{P}, \quad (2.2)$$

$$\frac{3}{2} \rho \frac{DT}{Dt} = -\mathbf{P} : \nabla \mathbf{u} - \nabla \cdot \mathbf{q} - \gamma, \quad (2.3)$$

where $D/Dt = \partial/\partial t + \mathbf{u} \cdot \nabla$ denotes the advective derivative, \mathbf{g} is the acceleration due to gravity, \mathbf{P} is the pressure tensor, \mathbf{q} is the flux of granular temperature (which we refer to as the heat flux) and γ is the dissipation due to inelastic collisions. Equations (2.1) and (2.2) are the familiar equations of mass and momentum conservation, respectively. Equation (2.3) represents the conservation of energy and describes the changes in the granular temperature due to the production by shear work (the term $-\mathbf{P}:\nabla\mathbf{u}$), the conduction ($-\nabla\cdot\mathbf{q}$), and dissipation in collisions ($-\gamma$).

Kinetic theory provides constitutive relations to close the system of governing equations by expressing the pressure tensor, the heat flux and dissipation as functions of the mean field variables. The constitutive theory of Lun *et al.* (1984) gives the pressure tensor and heat flux in the form

$$\mathbf{P} = (p - \xi(\nabla\cdot\mathbf{u}))\mathbf{I} - 2\eta\mathbf{S}, \quad (2.4)$$

$$\mathbf{q} = -K\nabla T + K^*\nabla v, \quad (2.5)$$

$$\mathbf{S} = \frac{1}{2}(\nabla\mathbf{u} + \nabla\mathbf{u}^T) - \frac{1}{3}(\nabla\cdot\mathbf{u})\mathbf{I} \quad (2.6)$$

where \mathbf{I} is the identity matrix and \mathbf{S} is the deviatoric part of the symmetric strain rate tensor, and where $v = \rho/\rho_p$ is the volume fraction with ρ_p the material density of a grain. The pressure tensor has the familiar form from Newtonian fluid mechanics, with the shear stresses linearly proportional to the strain rate. However, for a rapid granular flow the viscosity is dependent on the local density and granular temperature. The heat flux is a modified Fourier conduction law, with a term proportional to the gradient of v . The kinetic theory of Lun *et al.* (1984) results in $K^* \geq 0$, a diffusion along density gradients from diffuse to dense regions. In the studies of Forterre & Pouliquen (2002) and Mitarai & Nakanishi (2004), this additional term is discarded with the justification that it has little effect on the steady flow solutions but increases the algebraic complexity of the system. We retain this term in this study but investigate the effect of setting $K^* \equiv 0$ in the Appendix.

The pressure p , viscosity η , bulk viscosity ξ , conductivities K and K^* and the dissipation γ are given as functions of the volume fraction and granular temperature as

$$\left. \begin{aligned} p &= \rho_p g_1(v)T, & \eta &= \rho_p d g_2(v)T^{1/2}, & \xi &= \rho_p d g_6(v)T^{1/2}, \\ K &= \rho_p d g_3(v)T^{1/2}, & K^* &= \rho_p d g_4(v)T^{3/2}, & \gamma &= \frac{\rho_p}{d} g_5(v)T^{3/2}, \end{aligned} \right\} \quad (2.7)$$

where d is the grain diameter and the dependence on the volume fraction has been collected into dimensionless functions $g_i(v)$ given in table 1 (Lun *et al.* 1984), each of which depend on the radial distribution function $g_0(v)$. We employ the radial distribution function proposed by Lun & Savage (1986), as recalled in table 1, which diverges as the volume fraction approaches the maximum volume fraction v^* (we take $v^* = 0.62$ in the following analysis). The constitutive functions introduce the coefficient of restitution between particle collisions e , with $0 < e \leq 1$. Note that K^* is proportional to $1 - e$, so vanishes in the elastic limit, and γ is proportional to $1 - e^2$, the ratio of the pre-collision and post-collision kinetic energy of colliding grains. The kinetic theory of Lun *et al.* (1984) is appropriate for nearly elastic grains.

2.2. Boundary conditions

The governing equations are augmented with conditions to account for the effect of boundaries on the flow domain. Observations of granular flows show a slip velocity at solid walls, and shear work produces velocity fluctuations and a heating of the flow. However, inelastic collisions between flowing grains and the boundary wall dissipate

$$\begin{aligned}
 g_0 &= \left(1 - \frac{\nu}{\nu^*}\right)^{-5\nu^*/2} \\
 g_1 &= \nu [1 + 2(1 + e)\nu g_0] \\
 g_2 &= \frac{\sqrt{\pi}\nu(5 + 4(1 + e)\nu g_0)}{120(3 - e)(1 + e)\nu g_0} [5 + 2(1 + e)(3e - 1)\nu g_0] + \frac{4}{5\sqrt{\pi}}(1 + e)\nu^2 g_0 \\
 g_3 &= \frac{\sqrt{\pi}(5 + 6(1 + e)\nu g_0)}{4(1 + e)(49 - 33e)g_0} [5 + 3(1 + e)^2(2e - 1)\nu g_0] + \frac{2}{\sqrt{\pi}}(1 + e)\nu^2 g_0 \\
 g_4 &= \frac{3\sqrt{\pi}(5 + 6(1 + e)\nu g_0)}{4(49 - 33e)\nu g_0} e(1 - e) \frac{d}{d\nu}(\nu^2 g_0) \\
 g_5 &= \frac{12}{\sqrt{\pi}}(1 - e^2)\nu^2 g_0 \\
 g_6 &= \frac{4}{3\sqrt{\pi}}(1 + e)\nu^2 g_0
 \end{aligned}$$

TABLE 1. Dimensionless constitutive functions $g_i(\nu; e)$, including the radial distribution function $g_0(\nu; \nu^*)$.

kinetic energy. It is therefore possible to obtain a flow where the wall is a net source of granular temperature (which we refer to as a productive boundary) whereas in another situation the wall becomes a net sink of granular temperature (a dissipative boundary). While boundary conditions at solid walls have been proposed based on heuristic arguments (Johnson & Jackson 1987; Johnson *et al.* 1990), Richman (1988) derives boundary conditions based on the kinetic theory with assumptions consistent with the constitutive relations of Lun *et al.* (1984), and we adopt these boundary conditions in this study.

We consider a solid boundary, with an inward pointing unit normal \mathbf{n} , roughened by randomly fixing hemispherical grains. Such roughened boundaries are typical in experimental realizations (Forterre & Pouliquen 2002) to maintain an agitated flow at the wall. The roughness of the boundary is quantified in terms of the average spacing of the attached grains, s_w , and their diameter, d_w , through the boundary roughness parameter, r , defined by

$$r = \frac{s_w + d_w}{d + d_w}. \tag{2.8}$$

The boundary is roughened by increasing r , although the range of r is restricted to prevent grains making contact with the flat boundary. In the following we take $d_w = d$, so the grains attached to the wall have the same size as those within the flow, and r is restricted to $1/2 \leq r \leq \sqrt{3}/2$.

We define $\mathbf{u}_s = \mathbf{U} - \mathbf{u}$ to be the slip velocity, with \mathbf{U} the velocity of the boundary and \mathbf{u} the velocity of grains at the boundary. A balance of the momentum in the flow adjacent to the solid boundary with the momentum generated by the boundary gives

$$\mathbf{M} = \mathbf{P} \cdot \mathbf{n}, \tag{2.9}$$

where \mathbf{M} is the boundary traction force with components determined by Richman (1988) as

$$M_i = \rho_p \nu \chi T \left[n_i + \sqrt{\frac{2}{\pi}} \frac{u_{si}}{\sqrt{T}} \kappa + \sqrt{\frac{2}{\pi}} \frac{\bar{d}}{\sqrt{T}} \frac{\partial u_k}{\partial x_j} (A(\nu) \mathcal{J}_{ijk} + n_j \mathcal{J}_{ik}) \right], \tag{2.10}$$

where $\bar{d} = (d + d_w)/2$, κ is a function of the roughness parameter,

$$\kappa(r) = \frac{2}{3} \left(\frac{2}{1 + \sqrt{1 - r^2}} - \sqrt{1 - r^2} \right), \quad (2.11)$$

the function $A(v)$ is given by

$$A(v) = 1 + \frac{d\pi}{12\sqrt{2}\bar{d}} \left(1 + \frac{5}{8vg_0(v)} \right) \quad (2.12)$$

and the tensors \mathcal{I} and \mathcal{J} have components

$$\left. \begin{aligned} \mathcal{I}_{ik} &= (\kappa + 2\sqrt{1 - r^2})n_i n_k + \kappa(\tau_i \tau_k + t_i t_k), \\ \mathcal{J}_{ijk} &= (r^2 - 2)n_i n_j n_k - \frac{1}{2}r^2[n_i(\tau_j \tau_k + t_i t_k) + n_j(\tau_k \tau_i + t_k t_i) + n_k(\tau_i \tau_j + t_i t_j)], \end{aligned} \right\} \quad (2.13)$$

where the vectors \mathbf{n} , $\boldsymbol{\tau}$, \mathbf{t} form an orthonormal triad. The summation convention is employed in (2.10). The function χ is the ‘exclusion factor’ which accounts for the proportion of grains in the flow which cannot collide with the wall due to obstruction by other grains, and as yet remains undetermined.

An energy balance at the wall gives,

$$\mathbf{q} \cdot \mathbf{n} = \mathbf{M} \cdot \mathbf{u}_s - \mathcal{D}, \quad (2.14)$$

where \mathcal{D} is the dissipation of granular temperature due to collisions between flowing grains and the hemispheres attached to the boundary. If e_w is the coefficient of restitution characterizing these collisions, Richman (1988) determines the boundary dissipation as

$$\mathcal{D} = \sqrt{\frac{2}{\pi}} \frac{2(1 - e_w)}{1 + \sqrt{1 - r^2}} \rho_p v \chi T^{3/2}. \quad (2.15)$$

In the derivation of the macroscopic boundary closures from a micromechanical model of collisions between flowing grains and a bumpy boundary, Richman (1988) makes the assumption that collisions between flowing grains and the boundary are nearly elastic, which is consistent with the assumption of nearly elastic collisions in the derivation of the constitutive relations (Lun *et al.* 1984). In addition, Richman (1988) assumes that the slip velocity is small in comparison to the fluctuation velocity (given by $T^{1/2}$). In many of the solutions we obtain this condition is not strictly fulfilled. However, the careful derivation of the boundary conditions via a kinetic theory approach is preferred to the heuristic boundary conditions of Johnson & Jackson (1987).

In addition to the conditions at the solid boundary, we require boundary conditions to describe the free surface. In a rapid granular flow there is no material surface but a diffuse saltation layer of grains thrown from the main body of the flow. While the kinetic theory is strictly not appropriate in this regime, since the grains follow collisionless ballistic trajectories, several studies have applied the continuum model on a semi-infinite domain by employing asymptotic boundary conditions appropriate for vanishingly small volume fractions (Ahn *et al.* 1992; Azanza *et al.* 1999; Forterre & Pouliquen 2002; Mitarai & Nakanishi 2004). For the majority of the analysis conducted in this study, we employ the asymptotic free surface conditions and pose the continuum equations on a semi-infinite domain, demanding

$$\rho \rightarrow 0, \quad \mathbf{P} \rightarrow 0 \quad \text{and} \quad \mathbf{q} \cdot \hat{\mathbf{z}} \rightarrow 0 \quad \text{as} \quad z \rightarrow \infty, \quad (2.16)$$

where z represents the unbounded coordinate and $\hat{\mathbf{z}}$ the unit vector in that direction.

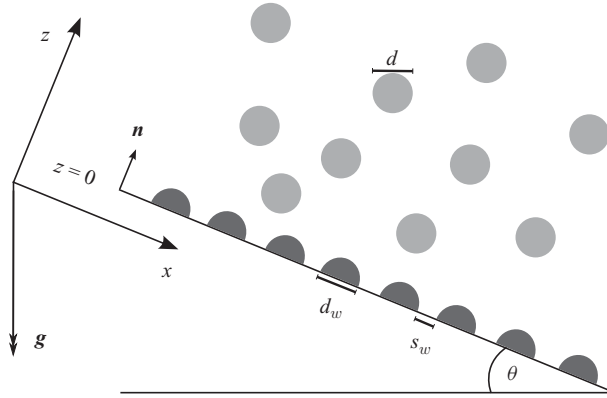


FIGURE 1. Coordinate system for a granular chute flow.

An alternative surface boundary condition has been derived by Jenkins & Hanes (1993) by identifying the point in the flow at which the mean free time between collisions equals the time for a grain thrown free of the collisional bulk to follow a ballistic trajectory and re-enter the bulk flow. The freely flying grain gains energy during the ballistic flight, and the interface becomes a source of heat for the collisional bulk flow. The conditions obtained by Jenkins & Hanes (1993), which we refer to as the interface surface conditions, specify the normal stress and the energy fluxes due to the overlaying freely flying grains (see §3.7). In §3.7 we examine the influence of the free surface conditions on the steady flow solutions, showing that the interface surface conditions result in only a small quantitative change in the solution profiles.

3. Steady, fully developed chute flows

3.1. Steady flow equations

We consider the gravity-driven free surface flow of grains down a planar chute inclined at an angle θ to the horizontal (figure 1). Dimensionless variables are formed by scaling lengths by the grain diameter d , time by $d(gd \cos \theta)^{-1/2}$ and density by the grain density ρ_p . In the following we use dimensionless variables. The transformation to dimensionless variables leaves four parameters which we identify as the particle–particle coefficient of restitution e , the particle–wall coefficient of restitution e_w , the boundary roughness r and the chute slope $\tan \theta$.

For steady, fully developed flow we seek solutions for the volume fraction, mean downslope velocity and granular temperature which are dependent only on z , the distance above the base, and for such a flow the mass conservation equation (2.1) is satisfied with $w \equiv 0$. The conservation of momentum (2.2) gives equations in the downslope and normal directions

$$\frac{dP_{xz}}{dz} = v \tan \theta, \quad (3.1)$$

$$\frac{dP_{zz}}{dz} = -v, \quad (3.2)$$

respectively, which can be combined and integrated immediately (employing the stress free condition at the free surface, $P_{xx} \rightarrow 0$ and $P_{xz} \rightarrow 0$ as $z \rightarrow \infty$) to obtain $P_{xz} = -\tan \theta P_{zz}$. We therefore obtain the Coulomb-like relationship between the shear and normal stresses through the flow. The heat flux in the fully developed flow

occurs only in the direction normal to the plane, so we set $\mathbf{q} = q\hat{z}$, and the equation of energy conservation (2.3) becomes

$$\frac{dq}{dz} = -P_{xz} \frac{du}{dz} - \gamma. \tag{3.3}$$

The constitutive relations of Lun *et al.* (1984), for the fully developed flow, reduce to

$$P_{xx} = P_{zz} = g_1 T, \tag{3.4}$$

$$P_{xz} = P_{zx} = -g_2 \sqrt{T} \frac{du}{dz}, \tag{3.5}$$

$$q = -g_3 T^{1/2} \frac{dT}{dz} + g_4 T^{3/2} \frac{dv}{dz}, \tag{3.6}$$

$$\gamma = g_5 T^{3/2}, \tag{3.7}$$

and on substituting these into (3.1)–(3.3) we obtain a system of ordinary differential equations:

$$\frac{d}{dz} (g_1 T) = -v, \tag{3.8}$$

$$\frac{d}{dz} \left(g_4 T^{3/2} \frac{dv}{dz} - g_3 T^{1/2} \frac{dT}{dz} \right) = \left(\frac{(g_1 \tan \theta)^2}{g_2} - g_5 \right) T^{3/2}, \tag{3.9}$$

$$\frac{du}{dz} = \frac{g_1 \tan \theta}{g_2} \sqrt{T}. \tag{3.10}$$

The equation for the mean velocity, (3.10), is decoupled and we show below that the boundary condition for the velocity is also decoupled. Thus the velocity field can be obtained once the solutions for the volume fraction and granular temperature fields are found.

The momentum balance at the base boundary, (2.9), gives two conditions,

$$M_x = P_{xz}, \tag{3.11}$$

$$M_z = P_{zz}, \tag{3.12}$$

and the components of the boundary traction force given by (2.10), for a fully developed chute flow, become

$$M_x = \sqrt{\frac{2}{\pi}} v \chi \sqrt{T} \left(\kappa u_s + \left(\kappa - \frac{1}{2} r^2 \right) \frac{du}{dz} \right), \tag{3.13}$$

$$M_z = v \chi T, \tag{3.14}$$

where $u_s = -u(0)$ since the boundary is stationary. The momentum balance normal to the base boundary (3.12) can then be used to determine the exclusion factor as $\chi(v) = g_1(v)/v$. By combining (3.10), (3.11) and (3.13) we find the slip velocity at the base boundary is given by

$$u_s = -F_1 \sqrt{T} \quad \text{at } z = 0, \tag{3.15}$$

where

$$F_1 = \frac{\tan \theta}{\kappa} \left(\sqrt{\frac{\pi}{2}} + \left(\kappa - \frac{1}{2} Ar^2 \right) \frac{g_1}{g_2} \right). \tag{3.16}$$

$g_0 = g_{00} + g_{01}\nu + \dots$	$g_{00} = 1$	$g_{01} = 5/2$
$g_1 = g_{11}\nu + \dots$	$g_{11} = 1$	
$g_2 = g_{20} + \dots$	$g_{20} = \frac{5\sqrt{\pi}}{24(3-e)(1+e)}$	
$g_3 = g_{30} + \dots$	$g_{30} = \frac{25\sqrt{\pi}}{4(1+e)(49-33e)}$	
$g_4 = g_{40} + \dots$	$g_{40} = \frac{15\sqrt{\pi}e(1-e)}{2(49-33e)}$	
$g_5 = g_{52}\nu^2 + \dots$	$g_{52} = \frac{12}{\sqrt{\pi}}(1-e^2)$	

TABLE 2. Leading asymptotic behaviour of the dimensionless constitutive functions $g_i(\nu; e)$, including the radial distribution function $g_0(\nu; \nu^*)$, for small volume fraction.

The energy balance at the base boundary is $q = M_x u_s - \mathcal{D}$, which can be written as

$$-g_3\sqrt{T}\frac{dT}{dz} + g_4T^{3/2}\frac{d\nu}{dz} = F_2T^{3/2} \quad \text{at } z = 0, \tag{3.17}$$

where

$$F_2 = g_1\sqrt{\frac{2}{\pi}}\left(\kappa F_1^2 - \frac{g_1 \tan \theta}{g_2}\left(\kappa - \frac{1}{2}Ar^2\right)F_1 - \frac{2(1-e_w)}{1+\sqrt{1-r^2}}\right). \tag{3.18}$$

3.2. Far-field asymptotic behaviour

At the free surface we impose the asymptotic conditions given by (2.16). Ahn *et al.* (1992) show that the no-stress condition in the far field is equivalent to demanding

$$\nu \rightarrow 0 \quad \text{and} \quad \frac{dT}{dz} \rightarrow 0 \quad \text{as } z \rightarrow \infty, \tag{3.19}$$

and in addition these conditions ensure vanishing heat flux, $q \rightarrow 0$ as $z \rightarrow \infty$.

The far-field behaviour of the steady flow solution can be determined by making an asymptotic expansion in the volume fraction $\nu \ll 1$ and heat flux $|q| \ll 1$, retaining only the leading terms in expansions of the governing equations and constitutive relations. Table 2 gives the leading-order forms of the dimensionless functions g_i for $\nu \ll 1$.

The asymptotic forms of (3.6), (3.8) and (3.9) are

$$\frac{d\nu}{dz} = -\frac{\nu}{T}, \tag{3.20}$$

$$\frac{dT}{dz} = \frac{g_{40}}{g_{30}}\nu - \frac{q}{g_{30}\sqrt{T}}, \tag{3.21}$$

$$\frac{dq}{dz} = \left(\frac{\tan^2 \theta}{g_{20}} - g_{52}\right)\nu^2 T^{3/2}, \tag{3.22}$$

so the temperature in the far field is constant at leading order, $T \rightarrow T_\infty$ as $z \rightarrow \infty$ where the far-field temperature T_∞ is undetermined. From (3.20)–(3.22) we obtain the behaviour of the volume fraction, granular temperature and heat flux in the

far field,

$$v = ae^{-z/T_\infty}, \tag{3.23}$$

$$T = T_\infty + \frac{g_{40}}{g_{30}} T_\infty a e^{-z/T_\infty}, \tag{3.24}$$

$$q = -\frac{1}{2} \left(\frac{\tan^2 \theta}{g_{20}} - g_{52} \right) T_\infty^{5/2} a^2 e^{-2z/T_\infty}, \tag{3.25}$$

where a is an undetermined constant. The fields decay exponentially in the far field, with the rate of decay fixed by the undetermined far-field granular temperature. Since the volume fraction vanishes in the limit $z \rightarrow \infty$ there is no heat content in the far field, even though the granular temperature is non-zero. Similar far-field behaviour, with the fields decaying exponentially with distance from the base, has been noted in previous studies (Johnson *et al.* 1990; Ahn *et al.* 1992; Azanza *et al.* 1999). There have also been studies of vibro-fluidized grain assemblies which have found exponential decay of the density and granular temperature as the free surface is approached (Kumaran 1998*a,b*; Brey, Ruiz-Montero & Moreno 2001).

The coupled ordinary differential equations, (3.8) and (3.9), are posed on a semi-infinite domain with the boundary condition (3.17) at the base ($z=0$) and the conditions (3.19) at the free surface (which is taken to be at infinity).

3.3. Macroscopic variables

It is clear that the trivial solution $v = 0, T = 0, u = 0$, satisfies the governing differential equations and boundary conditions and to obtain non-trivial solutions we must impose a further constraint. In chute flow experiments it is possible to specify the mass flux of material which is introduced onto the chute. On the semi-infinite domain the (dimensionless) mass flux is defined as

$$Q = \int_0^\infty v u \, dz, \tag{3.26}$$

and we seek solutions with a specified mass flux. It is also useful to characterize the solution in terms of the depth of the flowing layer, but the semi-infinite domain prevents an absolute notion of the depth. While the previous studies of Forterre & Pouliquen (2002) and Mitarai & Nakanishi (2004) adopt a cutoff in density to specify the flow depth, with the flow depth given as the height at which the density becomes 1 % of its maximum value within the flow, the choice of cutoff value is arbitrary. We therefore adopt the (dimensionless) centre-of-mass h as a measure of the flow depth which is defined as

$$h = \frac{1}{M} \int_0^\infty v z \, dz, \quad \text{where} \quad M = \int_0^\infty v \, dz. \tag{3.27}$$

In this expression M is the (dimensionless) mass hold-up, a measure of the mass of material within the flow. In discrete element simulations of granular chute flows the mass hold-up is typically used as the control variable rather than the mass flux. These depth-integrated variables provide well-defined measures of the depth and the mass of material flowing down the chute. To model chute flow experiments we impose the mass flux Q and augment the system of equations and boundary conditions with the integral constraint (3.26).

3.4. Numerical method

The system of ordinary differential equations is strongly nonlinear and non-trivial solutions must be obtained numerically. In the studies of Forterre & Pouliquen (2002)

and Mitarai & Nakanishi (2004) the basal volume fraction is fixed and a Runge–Kutta shooting method with domain truncation is employed to calculate solutions. However, an appropriate truncation point cannot be determined *a priori* when shooting from the base, and several iterations are required in order to converge to a solution which satisfies all the boundary conditions at the base and in the far field. Alternatively, we can specify the value of the granular temperature in the far field and integrate from an asymptotic far-field solution. However, the location of the base is then not known and we may not be able to satisfy the base boundary conditions, and thus an iterative adjustment of the ‘initial condition’ in the far field is required (Sellar 2003).

Rather than employ the shooting procedure, we develop a Chebyshev pseudospectral scheme (Boyd 2000) to solve numerically the system of ordinary differential equations to a high accuracy. The pseudospectral method provides a functional approximation of the solution which is useful for further investigation of the solutions, in particular, the linear stability analysis of the steady flows which we perform in part 2 of this paper. In addition, the boundary conditions at both the base and in the far field are enforced simultaneously during the integration of the governing equations, and we can easily incorporate the integral mass flux constraint. Furthermore, the pseudospectral scheme lends itself to parametric continuation, which allows us to efficiently track solutions on varying the controlling parameters. We couple the pseudospectral solution procedure to the ‘Pitcon’ parametric continuation algorithm (Rheinboldt 1986) to determine families of solutions as the mass flux is varied for fixed material parameters and fixed inclination angle.

A Chebyshev polynomial of degree n is defined as $T_n(x) = \cos(n \cos^{-1}(x))$ for $x \in [-1, 1]$ (Abramowitz & Stegun 1965). In order to apply a Chebyshev expansion to determine chute flow solutions, it is necessary to map the semi-infinite domain above the base boundary to the domain of the Chebyshev polynomials. We do this by introducing a mapping from the semi-infinite domain to the unit interval, taking $\zeta = e^{-z/L}$ where ζ is the independent variable in the computational space and L is an adjustable map parameter. While alternative mappings are possible, the exponential mapping is advantageous here as the physical variables themselves decay exponentially and we thus enforce to appropriate asymptotic behaviour, provided L is chosen appropriately, without requiring the placement of many collocation points in the region of exponential decay. The physical variables of volume fraction and granular temperature are transformed to computational variables with $v(z) = X(\zeta)^2$ and $T(z) = Y(\zeta)^2$, the squares taken to ensure the positivity of the physical fields. The computational variables are then expanded in a series of Chebyshev polynomials, truncated after $N + 1$ terms,

$$X(\zeta) = \sum_{n=1}^{N+1} a_n T_{n-1}(2\zeta - 1), \quad Y(\zeta) = \sum_{n=1}^{N+1} b_n T_{n-1}(2\zeta - 1), \quad (3.28)$$

and the expansion coefficients $\{a_n\}$ and $\{b_n\}$ are determined numerically by collocation. The collocation points in computational space are given by the zeros of $T_N(2\zeta - 1) = 0$, so are fixed in computational space for a given spectral truncation. The map parameter L determines the distribution of these collocation points in physical space and must be selected to ensure that the placement of collocation points adequately covers regions of rapid variation in the solution. Since the governing equations are nonlinear an iterative procedure is required to obtain the solution.

If the governing equations are analytic on the computational domain the Chebyshev spectral expansion coefficients decay exponentially (Boyd 2000) and this offers considerable computational efficiency. We can ensure the governing equations are

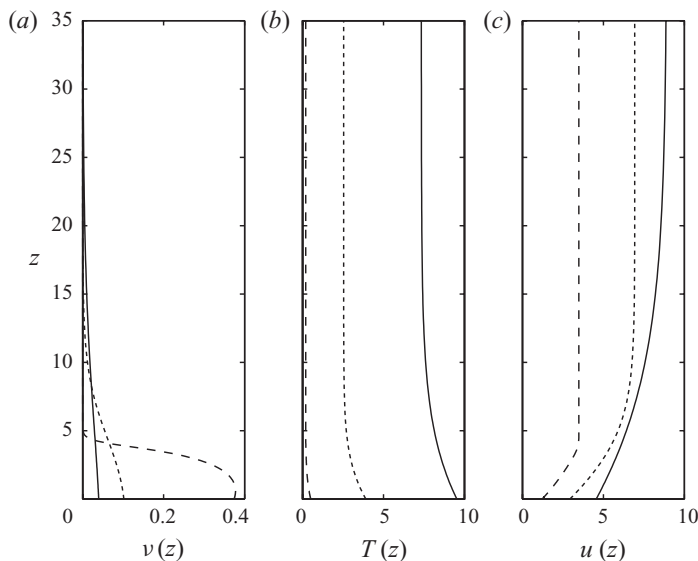


FIGURE 2. (a) Volume fraction profiles $v(z)$, (b) granular temperature profiles $T(z)$ and (c) velocity profiles $u(z)$ for three steady chute flows with mass flux $Q = 3$, with material parameters $e = e_w = 0.8$, $r = 0.6$ and a slope $\tan \theta = 0.3$. The flows are described as a high temperature, dilute flow (—) (A : $T_\infty = 7.34$, $h = 8.84$, $M = 0.44$), a mid-temperature flow (\cdots) (B : $T_\infty = 2.54$, $h = 3.98$, $M = 0.59$) and a low temperature, dense flow (---) (C : $T_\infty = 0.19$, $h = 1.77$, $M = 1.26$).

analytic through our choice of the map parameter L . An asymptotic analysis of the transformed governing equations around $\zeta = 0$ (corresponding to the limit $z \rightarrow \infty$ in physical space) shows the fields have the form

$$\left. \begin{aligned} X &\sim X_0 \zeta^{\alpha/2} + X_1 \zeta^{3\alpha/2} + X_2 \zeta^{5\alpha/2} + \cdots, \\ Y &\sim Y_0 + Y_1 \zeta^\alpha + Y_2 \zeta^{2\alpha} + \cdots, \end{aligned} \right\} \text{ for } \zeta \ll 1, \quad (3.29)$$

where $\alpha = L/T_\infty$ and $Y_0 = \sqrt{T_\infty}$. These series are consistent with the far-field behaviour of the fields determined above (3.23)–(3.24). The asymptotic series can be made analytic as $\zeta \rightarrow 0$ (so the fields are analytic on the whole computational domain) by taking

$$L = 2kT_\infty, \quad (3.30)$$

for $k \in \mathbb{N}$. Thus analyticity can be ensured if the far-field granular temperature is known. However, when imposing the mass flux (3.26) the far-field granular temperature is obtained as part of the solution and so we cannot ensure analyticity *a priori*. We therefore adjust the map parameter during the solution process, and our freedom in selecting the map parameter is through the choice of the integer k .

3.5. Results

For fixed material parameters steady solutions are found only for a finite range of inclination angles (Anderson & Jackson 1992; Forterre & Pouliquen 2002). The domains in the parameter space for which steady solutions can be found are examined in §4. Here we investigate the character of the solutions and the influence of the controlling parameters. We begin by fixing the material parameters, taking $e = e_w = 0.8$ and $r = 0.6$, and fixing the chute slope at $\tan \theta = 0.3$.

Imposing a mass flux of $Q = 3$ we find that three solutions are possible, as shown in figure 2. The flows can be categorized, using the granular temperature in the far field,

as high, mid- and low temperature flows, or by using the depth-integrated variables of mass hold-up and centre-of-mass. The high temperature flow, which has a far-field granular temperature $T_\infty = 7.34$, is dilute and deep, with a mass hold-up $M = 0.44$ and centre-of-mass $h = 8.84$. The low temperature flow has far-field temperature $T_\infty = 0.19$ and is dense and shallow, with $M = 1.26$ and $h = 1.77$, and shows a density inversion in the volume fraction profile. The mid-temperature flow has a far-field granular temperature $T_\infty = 2.54$ lying intermediate between the high and low temperature flows and has $M = 0.59$ and $h = 3.98$. However, the mid-temperature flow here more closely resembles the high temperature profiles, with a monotonically decaying volume fraction.

With increasing density we observe in figure 2(c) a decrease in the slip velocity at the base. This reduces the shear work production of fluctuation energy and results in a decrease in the granular temperature throughout the flow depth. However, for this choice of material parameters the production of fluctuation energy at the base is always larger than the loss due to inelastic collisions between the flowing grains and the solid boundary, and the granular temperature profiles have a maximum at the base. As there is no flux of granular temperature through the surface, the fluctuation energy produced at the base must be dissipated by collisions in the flowing grain assembly. The interior flow must then be a net energy sink, and we therefore refer to such flows as dissipative. For alternative material parameters the base boundary becomes an energy sink and the collisional flow must be a net source of granular temperature, so the flow is productive. We discuss productive flows in §3.6.

The features seen in these flows are similar to those calculated by Forterre & Pouliquen (2002) with a model employing different boundary conditions and with a different choice material parameters, suggesting the qualitative character of the solutions is robust to changes in the governing equations. However, Forterre & Pouliquen (2002) did not report multiple solutions for fixed control parameters. Furthermore, we show in the Appendix that the form of the heat flux has little effect on the profiles and the multiple solutions persist if a Fourier form of the heat flux is employed rather than the modified Fourier form we adopt.

Multiple solutions were reported by Johnson *et al.* (1990), Nott & Jackson (1992) and Anderson & Jackson (1992) in their studies on rapid granular flows on inclined planes. However, these studies found only two solutions for a specified volume flux of material, unless a frictional contribution was included in the constitutive relations giving rise to a third solution (Anderson & Jackson 1992). In contrast, we find three solutions can be obtained for a fully-collisional rapid granular flow model. The third solution is a dilute and relatively deep flow and a highly accurate numerical scheme is required to obtain this solution branch. The pseudospectral method developed here specifically maps the flow domain onto the unit interval and makes use of the low volume fraction asymptotic form of the solutions in the far field; it is thus well suited to obtaining these dilute solutions.

The flow solutions in figure 2 are found using parametric continuation to vary the mass flux and trace the family of solutions for fixed material parameters. The relationships between the macroscopic depth-integrated variables for a family of solutions is shown in figure 3, for a slope $\tan \theta = 0.3$. When specifying the mass flux of material and measuring the flow depth, defined here as the centre-of-mass, or mass of material, defined as the mass hold-up, we find a region where multiple solutions can be obtained, with three solutions of equal mass flux. Outside of this region we find a unique solution for a specified mass flux. If instead the mass hold-up is specified there is a one-to-one relationship with the centre-of-mass. However, in experimental chute

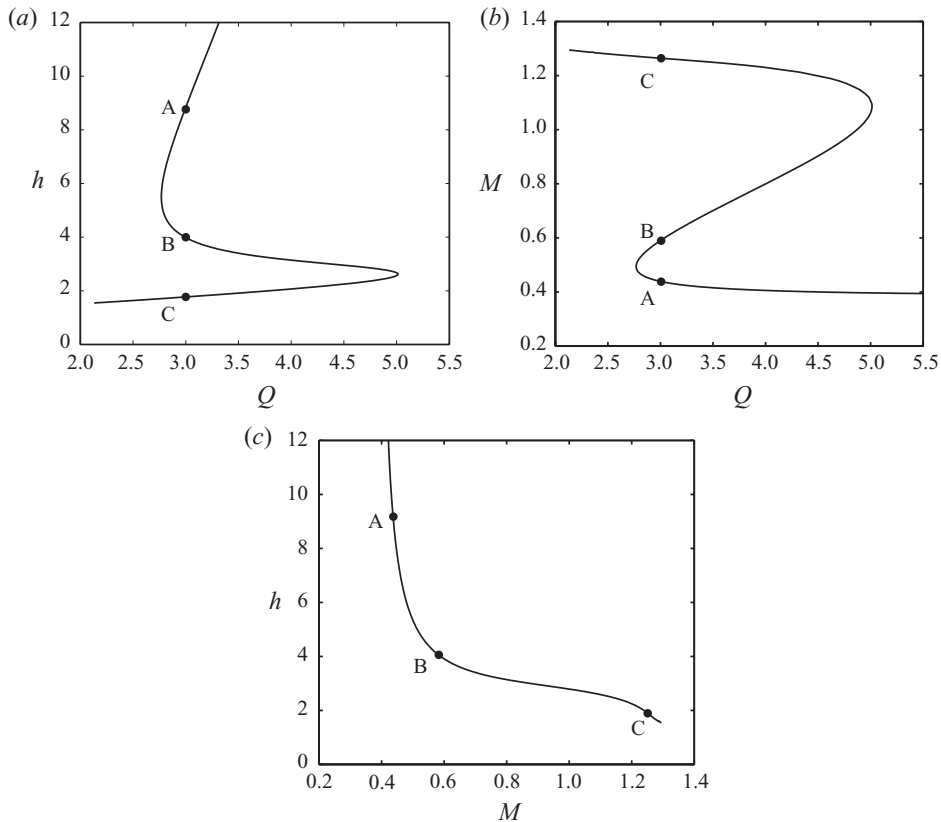


FIGURE 3. (a) Centre-of-mass h as a function of mass flux Q , (b) mass hold-up M as a function of mass flux Q and (c) centre-of-mass h as a function of mass hold-up M for steady, fully developed rapid granular flows on a chute with slope $\tan \theta = 0.3$ and material parameters $e = e_w = 0.8$, $r = 0.6$. Points labelled on the curves correspond to the flows in figure 2.

flows the mass of material on the chute cannot be directly controlled, rather the mass flux of material down the chute is fixed at the point of release. We therefore prefer to consider the mass flux of material as the natural control parameter for chute flows. Multiple solutions for a specified mass flux are also found when employing a cutoff height to quantify the flow depth rather than the depth-integrated centre-of-mass.

The three branches on the Q - h and Q - M curves can be distinguished with reference to the magnitude of the far-field granular temperature, as with the categorization of the three solution profiles in figure 2. The high temperature branch has flows which are deep and dilute, such as the high temperature flow in figure 2 which is marked as A in figure 3. The solutions on the low temperature branch, such as the low temperature flow in figure 2 which is marked as C in figure 3, are shallow and relatively dense. The mid-temperature branch has solutions which are intermediate between these two, for example, the mid-temperature flow in figure 2 which is marked as B in figure 3. The three solution branches are also found if interface surface conditions are employed rather than the asymptotic surface conditions, as demonstrated in §3.7.

We consider now the influence of the inclination angle of the chute on the macroscopic flow behaviour, focusing on the relationship between the centre-of-mass and the imposed mass flux of material, as shown in figure 4 for fixed material

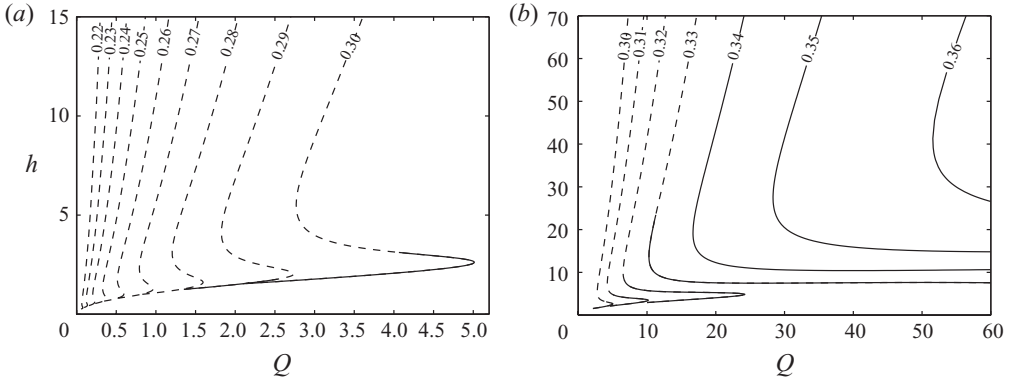


FIGURE 4. The centre-of-mass h as a function of mass flux Q for chutes slopes in the range (a) $\tan \theta \in [0.22, 0.3]$ and (b) $\tan \theta \in [0.3, 0.36]$, for fixed material parameters $e = e_w = 0.8$ and $r = 0.6$. Solid lines indicate steady solutions which exhibit a density inversion, whereas dashed lines indicate solutions with monotonic volume fraction profiles.

parameters, $e = e_w = 0.8$ and $r = 0.6$. For these parameter values the base boundary remains a source of fluctuation energy for all inclination values for which steady solution can be found. On the gentle chute slopes in figure 4(a) a region of multiple flow solutions for a specified mass flux occurs for all inclination angles, with the size of this region increasing as the slope becomes steeper. On further increasing the slope angle, as shown in figure 4(b), we observe a qualitative change in the relationship. For sufficiently steep slopes, here $\tan \theta > 0.33$ giving an inclination angle of $\theta > 18^\circ$, we can no longer find three flow solutions at equal mass flux. Instead there is a minimum mass flux at which steady flows are possible and above this minimum value we always find two solutions for a specified mass flux. Furthermore, the mass flux and flow depth are each increasing as the granular temperature approaches zero on the steep slopes ($\tan \theta > 0.33$) (this behaviour is not shown in figure 4), whereas the mass flux and flow depth approach zero at low granular temperature on the gentle slopes. Forterre & Pouliquen (2002) also noted a qualitative change in behaviour which occurs at an inclination angle of 18° when characterizing flows using the flow depth and mean density. However, in view of the different constitutive relations and boundary conditions, the concurrence of the inclination angles may be fortuitous.

We also display in figure 4 steady flows which exhibit a density inversion, where the maximum volume fraction occurs above the base boundary. For gentle slopes, with a chute slope $\tan \theta < 0.29$ no solutions are found which have a density inversion. On increasing the chute slope we find density inverted solutions if the flow depth is sufficiently small. On further increasing the chute inclination, we find that all solutions that we obtain display a density inversion for $\tan \theta > 0.333$. The presence of a density inversion has been proposed as a cause of instability in the steady chute flow (Forterre & Pouliquen 2002). In part 2 of this paper we investigate further the linear stability of the steady flows and the role of density inversions in the steady profiles and find no correlation between linear instability and density inversion in the underlying steady solution.

3.6. Productive flows

On varying the material parameters we can obtain steady flows for which the shear work in the interior of the flow dominates inelastic dissipation and there is a net production of fluctuation energy. In order to achieve an energy balance the base

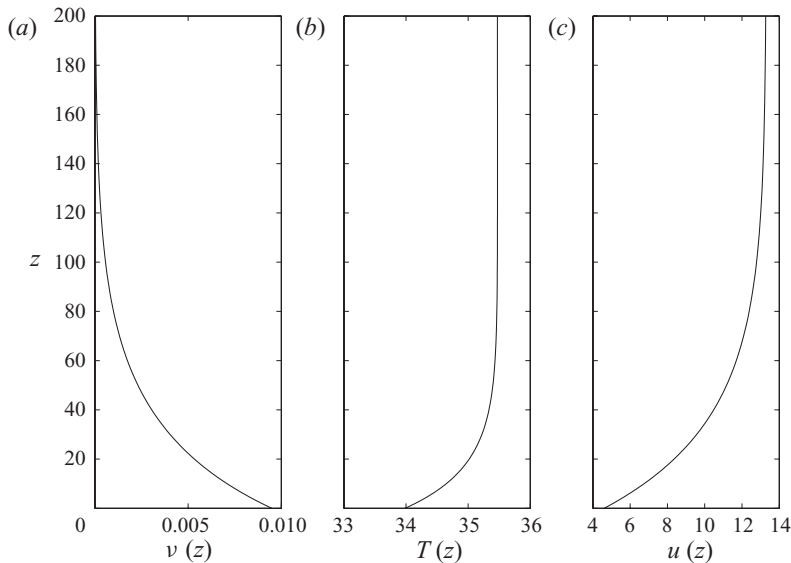


FIGURE 5. (a) Volume fraction profiles $v(z)$, (b) granular temperature profiles $T(z)$ and (c) velocity profiles $u(z)$ for a productive steady chute flows with mass flux $Q=3$, with material parameters $e=0.9$, $e_w=0.6$, $r=0.8$ and a slope $\tan\theta=0.4$.

boundary must dissipate the excess energy. While it is difficult to determine in advance the appropriate parameter values to achieve a productive flow (see §4), we can predict that it will be necessary to increase the coefficient of restitution in particle–particle collisions e , and decrease the coefficient of restitution in particle–wall collisions e_w . By taking $e=0.9$, $e_w=0.6$ and $r=0.8$ we find productive steady flows for a range of inclination angles, typically at steeper slopes than found for dissipative flows.

An example of a productive flow solution is shown in figure 5, where the flow parameters are $e=0.9$, $e_w=0.6$ and $r=0.8$, and the chute slope is $\tan\theta=0.4$. The striking difference with dissipative flows is the increase in granular temperature with distance from the base. However, as shown in the asymptotic form of the granular temperature at large heights in (3.24), the granular temperature must decay to its far-field value from above, so for productive flows the maximum granular temperature occurs in the interior of the flow. This feature is seen in a close inspection of the granular temperature profile.

The relationship between the macroscopic centre-of-mass h and mass flux Q for productive flows on a range of chute slopes is shown in figure 6, and is seen to be markedly different from the corresponding relationship for a dissipative parameter set. In particular, for these chute slopes we do not observe any multiplicity in the solutions, but a one-to-one relationship between the centre-of-mass and mass flux. It is possible to obtain productive flows on more gentle slopes, and here multiplicity is seen. However, for productive flows the multiplicity is found only in a small part of parameter space.

3.7. Interface surface boundary conditions

The asymptotic surface boundary conditions impose the governing equations on a semi-infinite domain, with the form of the governing equations at small volume fraction ensuring that the stresses and energy flux vanish as $z \rightarrow \infty$. However, in this extremely dilute flow the kinetic theory description of the motion may not be

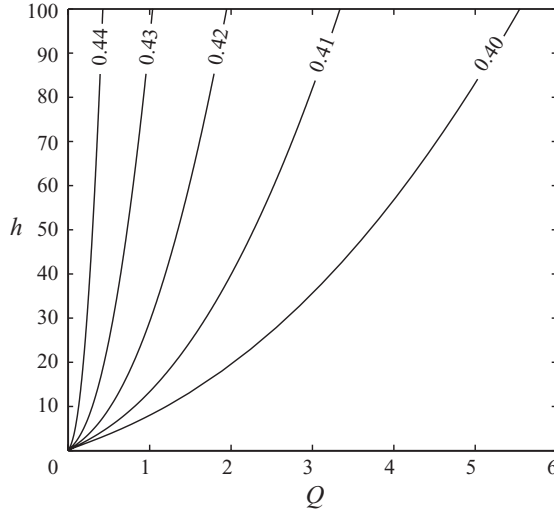


FIGURE 6. The centre-of-mass h as a function of mass flux Q for chute slopes in the range $\tan \theta \in [0.4, 0.44]$, for fixed material parameters $e = 0.9$, $e_w = 0.6$ and $r = 0.8$. For this parameter set, the flows are productive in the interior and the base is dissipative.

appropriate. An alternative surface condition, proposed by Jenkins & Hanes (1993), imposes a balance between the collisional stresses and energy flux in the bulk flow with those in an overlying saltation zone consisting of collisionless freely flying grains. The surface of the collisional flow is taken to be the interface between the collisional bulk and the freely flying grains.

We define $z = H$ to be the height of this interface for a steady, fully developed granular chute flow, noting that H must be determined as part of the solution. At the interface a balance of the collisional mean free time and the duration of a ballistic flight of a grain thrown from the interface provides a normal stress condition which, in the dimensionless variables appropriate to the chute flow, specifies (Jenkins & Hanes 1993)

$$p = \sqrt{\pi}/48. \quad (3.31)$$

The freely flying grains are accelerated under gravity and so gain energy during their ballistic flight. This energy is transferred to the collisional bulk when the grain impacts with grains at the interface, so the saltating grains heat the collisional flow. The heat flux at the interface, in the dimensionless variables is (Jenkins & Hanes 1993)

$$q = -p\sqrt{T} \tan^2 \theta. \quad (3.32)$$

Note $q < 0$ at the surface which represents a downward heat flux into the collisional bulk.

The interface conditions supplement the base boundary condition and the third-order system of equations. However, the location of the interface remains undetermined and to fully specify the problem we require an additional constraint; here we impose the mass flux of material. The governing equations are solved using a Chebyshev pseudospectral method, similar to that used when asymptotic conditions are imposed, except that here the equations are posed on a finite domain and an exponential mapping is not required. In figure 7 the volume fraction profiles of the three solutions found with mass flux $Q = 3$ are shown, together with the

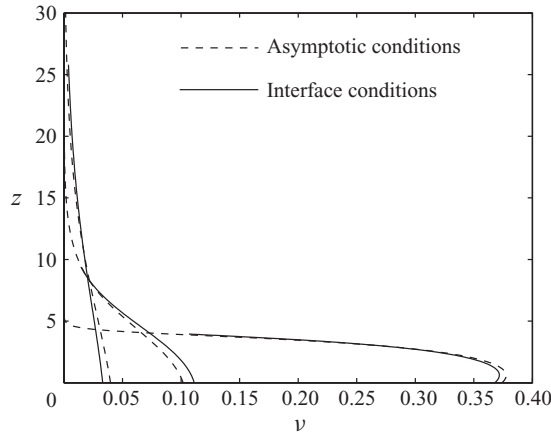


FIGURE 7. Volume fraction profiles for steady flow solutions with mass flux $Q = 3$ with interface surface conditions and the corresponding profiles with asymptotic conditions. The chute slope is $\tan \theta = 0.3$ and the flow parameters are $e = e_w = 0.8$, $r = 0.6$.

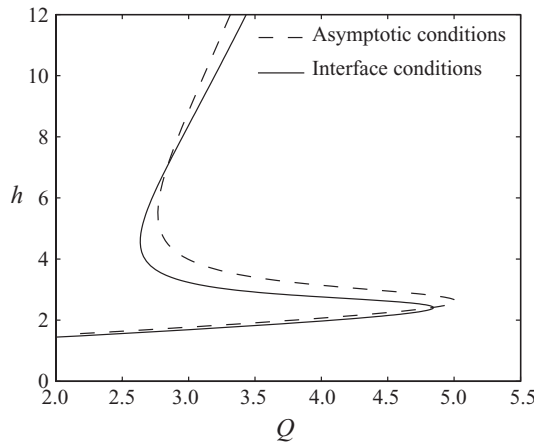


FIGURE 8. The centre-of-mass h as a function of mass flux Q with interface surface conditions and the corresponding relationship with asymptotic conditions enforced. The chute slope is $\tan \theta = 0.3$ and the flow parameters are $e = e_w = 0.8$, $r = 0.6$.

corresponding profiles obtained when asymptotic surface conditions are imposed. The profiles obtained with interface conditions share the same qualitative features as the profiles on the semi-infinite domain, and the form of the surface boundary condition has only a small influence on the solution profiles.

Similarly, the qualitative features of the macroscopic variables used to characterize the flows are relatively unaffected by the form of the surface boundary conditions. This is seen in figure 8, where the relationships between the centre-of-mass and the imposed mass flux are shown for a chute with slope $\tan \theta = 0.3$ with either the asymptotic or interface conditions enforced. We note in particular that the form of the surface boundary condition has little influence on the Q - h relationship on the low temperature branch, where the flow is dense and shallow.

In figure 9 we investigate the Q - h curves as the chute slope is varied. Comparing with figure 4 where the asymptotic surface conditions are applied, we see that much

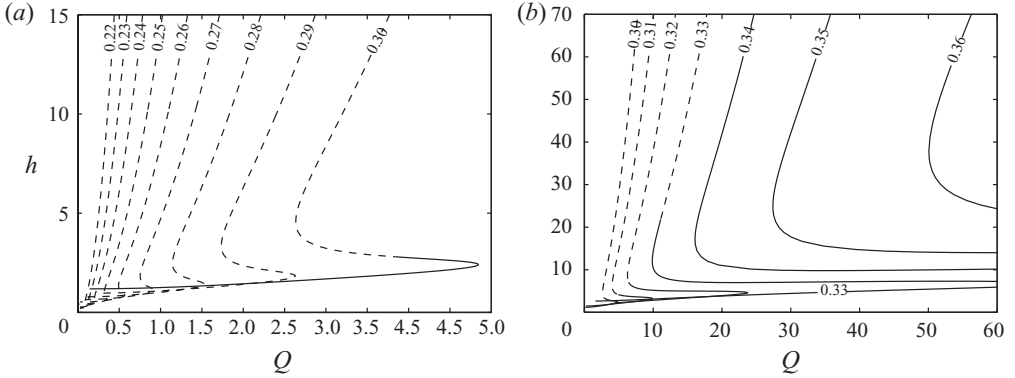


FIGURE 9. The centre-of-mass h as a function of mass flux Q for chute slopes in the range (a) $\tan \theta \in [0.22, 0.3]$ and (b) $\tan \theta \in [0.3, 0.36]$, for fixed material parameters $e = e_w = 0.8$ and $r = 0.6$, with interface surface boundary conditions. Solid lines indicate steady solutions which exhibit a density inversion, whereas dashed lines indicate solutions with monotonic volume fraction profiles.

of the behaviour is reproduced when we employ interface conditions. In particular, we observe the transition from solution curves where there is a region with three steady flow solutions with equal mass flux at gentle inclinations ($\tan \theta \leq 0.33$) to solution curves with a minimum mass flux, and with two solutions of equal mass flux above this minimum value, on steeper chutes ($\tan \theta \geq 0.34$). However, the interface boundary conditions do slightly change the transition from density inverted steady flows to flows with monotonic volume fraction profiles. In particular, when asymptotic surface conditions are employed there are density inverted flows for a chute slope $\tan \theta = 0.29$ whereas no density inverted flows are found for this chute slope when the interface conditions are used.

The qualitative features of the steady, fully developed rapid granular flows are seen to be insensitive to the form of the surface boundary conditions. However, we note that the interface conditions result in a finite domain on which the governing equations are defined (although the location of the interface is not known *a priori*), which is an advantage in the numerical solution of the nonlinear system of equations. The pseudospectral expansion on the finite domain converges exponentially quickly, and we find that many fewer Chebyshev polynomials are required in solving the system to a specified tolerance with interface conditions than are required for the corresponding system with asymptotic conditions (where we introduce an exponential mapping of the semi-infinite domain).

4. Domains of existence and high temperature asymptotic solutions

It has been shown that steady, fully developed solutions of the kinetic theory continuum model for rapid granular flows can only be found for a limited range of inclination angles (Anderson & Jackson 1992; Forterre & Pouliquen 2002). However, it is not known how the material parameters control this domain of existence, so it is not possible to predict in advance of any computation whether steady, fully developed solutions can be found for a given set of parameters, but the determination of the domains in which solutions exist using the full system of equations is a computationally expensive task. In this section we tackle this task by analysing the governing equations in the regime of high granular temperature to obtain a system

of equations containing a single controlling parameter and we are able to predict the regions in parameter space where steady solutions can be obtained.

Anderson & Jackson (1992) analysed the collisional theory of Haff (1983), using the high-density limit of the constitutive relations of Lun *et al.* (1984) to determine the unknown functions, under the assumption that the volume fraction of particles is high throughout the entire flow depth. Although this assumption fails as the free surface is approached, Anderson & Jackson (1992) were able to derive analytical solutions to the simplified equations and predict domains in parameter space where solutions of their full collisional theory could be obtained. Their analysis resulted in parameter groups which determined the nature of the energy balance within the flows and the effects of the boundary. Our asymptotic analysis results in parameter groups which share some of the characteristics of those determined by Anderson & Jackson (1992). In addition we are able to predict the qualitative change in the character of the density profiles (see figure 4), where there is a transition from high temperature flows where the volume fraction decreases monotonically with increasing distance from the base to high temperature flows which exhibit a density inversion.

4.1. Leading-order equations for high temperature flows

We analyse the governing equations in the regime of high temperature throughout, $T \gg 1$, to derive a reduced system with a single residual dimensionless parameter. To this end it is convenient to use $\epsilon = 1/T_\infty \ll 1$ as an ordering parameter and introduce $T = \tau/\epsilon$, where τ is order unity throughout. We anticipate, and confirm later, that the regime of high temperature also corresponds to dilute flows ($\nu \ll 1$). Therefore we may simplify the constitutive functions, given in table 1, to their leading-order forms,

$$g_1 \sim \nu, \quad g_2 \sim g_{20}, \quad g_3 \sim g_{30}, \quad g_4 \sim g_{40}, \quad g_5 \sim g_{52}\nu^2, \quad (4.1)$$

where g_{20}, g_{30}, g_{40} and g_{52} are functions of the coefficient of restitution, as given in table 2. In addition the boundary functions F_1 and F_2 are similarly approximated by their leading-order forms, so that $F_1 \sim F_{10}$, $F_2 \sim F_{21}\nu$ where

$$F_{10} = \frac{\tan \theta}{\kappa} \left(\sqrt{\frac{\pi}{2}} - \frac{1}{2}A_0r^2g_{20} \right), \quad (4.2)$$

$$F_{21} = \sqrt{\frac{2}{\pi}} \left(\frac{\pi \tan^2 \theta}{2 \kappa} - \sqrt{\frac{\pi}{2}} \frac{\tan^2 \theta}{2\kappa g_{20}} A_0r^2 - \frac{2(1 - e_w)}{1 + \sqrt{1 - r^2}} \right), \quad (4.3)$$

and where

$$\kappa(r) = \frac{2}{3} \left(\frac{2}{1 + \sqrt{1 - r^2}} - \sqrt{1 - r^2} \right), \quad A_0 = \frac{5\pi}{96\sqrt{2}}. \quad (4.4)$$

The parameter F_{21} determines the direction of the heat flux at the base boundary for the high temperature flow, with a productive boundary (i.e. a production of granular temperature at the boundary which is transported into the interior) if $F_{21} > 0$, and a dissipative boundary if $F_{21} < 0$.

In order to make an asymptotic analysis of the governing equations, we introduce a change of coordinate to the computational domain via the mapping

$$s = \exp(-z/T_\infty) = \exp(-\epsilon z). \quad (4.5)$$

From the far-field asymptotic analysis of §3.2, we note that the fields behave as polynomials as $s \rightarrow 0$. Here we seek an asymptotic approximation to the fields which is applicable over the entire domain, $s \in [0, 1]$.

The governing equations, in the scaled variables and transformed onto the finite computational domain, are, to leading order in ϵ and ν ,

$$s \frac{d}{ds} (\nu \tau) = \nu, \tag{4.6}$$

$$s \frac{d}{ds} \left(\frac{2g_{30}}{3} s \frac{d}{ds} (\tau^{3/2}) - g_{40} \tau^{3/2} s \frac{d\nu}{ds} \right) = \delta \epsilon^{-2} \nu^2 \tau^{3/2}, \tag{4.7}$$

subject to the energy base boundary condition

$$g_{30} \frac{d\tau}{ds} - g_{40} \tau \frac{d\nu}{ds} = F_{21} \epsilon^{-1} \nu \tau \quad \text{at } s = 1, \tag{4.8}$$

and the free surface conditions which demand $\nu \rightarrow 0$ and $\tau \rightarrow 1$ as $s \rightarrow 0$. The parameter

$$\delta = g_{52} - \frac{\tan^2 \theta}{g_{20}} \tag{4.9}$$

in (4.7) represents the local competition between dissipation and production of granular temperature within the interior of the flow. If $\delta > 0$ the dissipation exceeds the production throughout the high temperature flow and so the boundary must be a net source of energy in order to maintain the flow. On the other hand, if $\delta < 0$ the flow is productive, with energy production exceeding dissipation throughout and so a dissipative boundary is required. A distinguished scaling for (4.7) is found by setting $\nu = \alpha \epsilon \psi$, where ψ is an order 1 quantity and

$$\alpha = \frac{2g_{30}}{3F_{21}}. \tag{4.10}$$

We then obtain, to leading order in ϵ ,

$$s \frac{d}{ds} (\psi \tau) = \psi, \tag{4.11}$$

$$\lambda s \frac{d}{ds} \left(s \frac{d}{ds} (\tau^{3/2}) \right) = \psi^2 \tau^{3/2}, \tag{4.12}$$

subject to

$$\frac{d}{ds} (\tau^{3/2}) = \psi \tau^{3/2} \quad \text{at } s = 1, \tag{4.13}$$

and $\psi \rightarrow 0$, $\tau \rightarrow 1$ as $s \rightarrow 0$. We are left with a single parameter

$$\lambda = \frac{3F_{21}^2}{2g_{30}\delta}, \tag{4.14}$$

which is a function of the controlling parameters e , e_w , r and $\tan \theta$. Note that $\lambda > 0$ if the high temperature flow is dissipative, and $\lambda < 0$ if the high temperature flow is productive. Although this reduced system now only contains a single dimensionless parameter, rather than the four parameters of the full system, the approximate equations remain nonlinear and no analytic solution can be found.

We can obtain an asymptotic approximation to the velocity field, appropriate to high temperature flows, by taking the leading-order form of the decoupled velocity equation. We first transform to the computational domain and use the leading-order form of the constitutive functions to obtain

$$\epsilon s \frac{du}{ds} = -\frac{\tan \theta}{g_{20}} \epsilon \nu \frac{\tau^{1/2}}{\epsilon^{1/2}}, \tag{4.15}$$

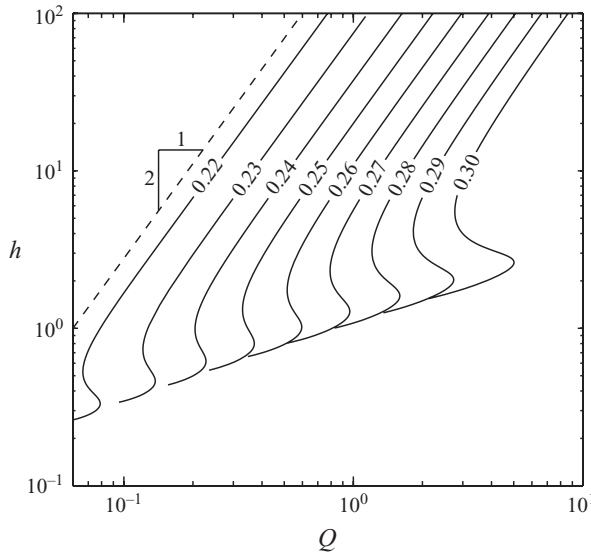


FIGURE 10. The centre-of-mass h as a function of mass flux Q on logarithmic axes, for chute slopes in the range $\tan \theta \in [0.22, 0.3]$, for fixed material parameters $e = e_w = 0.8$ and $r = 0.6$. On the high temperature branch the curves become parallel to a line with slope 2 (shown as the dashed line), indicating that $h \sim Q^2$ at sufficiently high temperatures.

with $u = \epsilon^{-1/2} F_{10} \tau^{1/2}$ at $s = 1$. We make the scaling $u = \epsilon^{-1/2} F_{10} U$ and obtain

$$s \frac{dU}{ds} = -\mu \psi \tau^{1/2}, \quad \text{where} \quad \mu = \frac{\alpha \tan \theta}{F_{10} g_{20}}. \tag{4.16}$$

The boundary condition for the slip velocity is

$$U = \tau^{1/2} \quad \text{at} \quad s = 1. \tag{4.17}$$

We can therefore recover the high temperature velocity field once solutions of (4.11) and (4.12) are known.

The scalings introduced when forming the high temperature asymptotic system directly show that the macroscopic flow variables, for high temperature, are approximated by

$$Q = \int_0^\infty v u \, dz = \epsilon^{-1/2} \alpha F_{10} \int_0^1 \frac{\psi U}{s} \, ds, \tag{4.18}$$

$$M = \int_0^\infty v \, dz = \alpha \int_0^1 \frac{\psi}{s} \, ds, \tag{4.19}$$

$$h = \frac{1}{M} \int_0^\infty v z \, dz = -\epsilon^{-1} \frac{\alpha}{M} \int_0^1 \frac{\psi \log s}{s} \, ds. \tag{4.20}$$

The asymptotic analysis therefore suggests that the centre-of-mass scales as $h \sim Q^2$ if the granular temperature is sufficiently high. This scaling is observed in the solutions of the full system of equations, as demonstrated in figure 10 for dissipative flows on relatively gentle inclines. In comparison, the centre-of-mass of a steady viscous incompressible Newtonian fluid flowing down an inclined plane scales as $h \sim Q^{1/3}$. The Bagnold scaling, which gives the shear stress proportional to the square of the

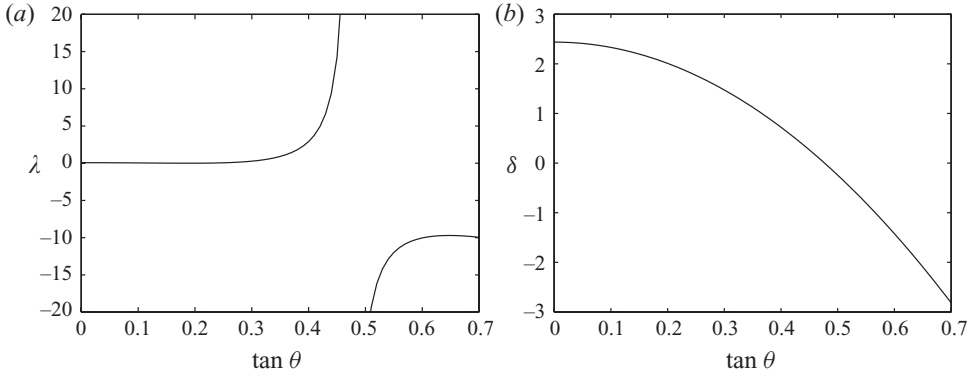


FIGURE 11. The parameters λ and δ as functions of the chute slope for flow parameters $e = e_w = 0.8$ and $r = 0.6$. Note that λ diverges as $\delta \rightarrow 0$. The parameter δ represents the competition between production by shear work and dissipation by inelastic collisions of fluctuation energy in the interior of the high temperature flow, with the high temperature flow dissipative if $\delta > 0$ and productive if $\delta < 0$.

velocity gradient, when applied to a granular chute flow with constant density results in the relation $h \sim Q^{2/5}$.

4.2. Approximate solutions for high temperature flows

In figure 11 we show the parameters λ and δ as functions of $\tan \theta$ for flow parameters $e = e_w = 0.8$ and $r = 0.6$. We see that, for gentle slopes, the parameter $|\lambda| \ll 1$ (with $|\lambda| < 1$ for $\tan \theta < 0.354$). Therefore, for sufficiently gentle slopes, the quantity λ can be taken as a small parameter within an asymptotic approximation of the solution. Furthermore $|\lambda| \ll 1$ represents a regular perturbation to the equivalent system with $\lambda = 0$ (note that taking $\phi = 0$, $\tau = 1$ satisfies (4.11), (4.12) and (4.13) when $\lambda = 0$, so $|\lambda| \ll 1$ is not a singular perturbation) and we can readily obtain an approximate solution via a regular perturbation expansion. For $|\lambda| \ll 1$ we find the approximate solution,

$$\psi = 2s\lambda + (s - 2s^3)\lambda^2 + O(\lambda^3), \quad (4.21)$$

$$\tau = 1 + \frac{2}{3}s^2\lambda + \left(\frac{2}{3}s^2 - \frac{5}{18}s^4\right)\lambda^2 + O(\lambda^3), \quad (4.22)$$

$$U = F_{10} + \left(2\mu(1-s) + \frac{1}{3}F_{10}\right)\lambda + \left(\frac{5}{9}\mu - \left(s - \frac{4}{9}s^3\right)\mu + \frac{5}{36}F_{10}\right)\lambda^2 + O(\lambda^3). \quad (4.23)$$

An example of the profiles obtained from the reduced system of equations describing high temperature flows, obtained from the regular perturbation expansion including terms up to λ^2 , is shown in figure 12, together with a numerically determined solution to the full nonlinear system of equations (3.8)–(3.10). When the parameter λ in the system of equations for high temperature flows cannot be considered asymptotically small the system (4.11)–(4.12) must be solved numerically. We use here a Runge–Kutta integration to solve the high temperature system of equations. Note that the point $s = 0$ is a regular singular point and by making a local series expansion in the neighbourhood of this point we can generate an initial condition for the Runge–Kutta integration. This analysis gives the conditions

$$\psi \sim cs, \quad \tau \sim 1 + \frac{c^2s^2}{6\lambda}, \quad \tau' \sim \frac{c^2s}{3\lambda}, \quad (4.24)$$

for $s \ll 1$, which we enforce as initial conditions at a small distance from the singular point at $s = 0$. The constant $c > 0$ remains undetermined by the local analysis. With an arbitrary value for c the Runge–Kutta method can be used to integrate the

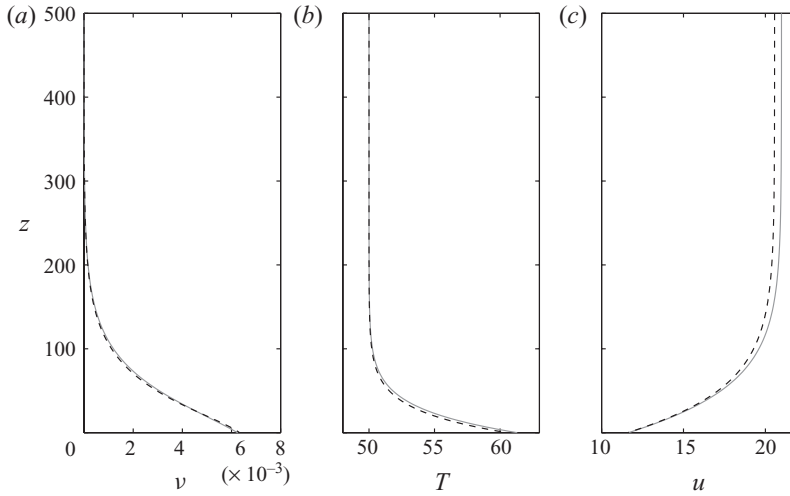


FIGURE 12. Comparison of an approximate solution (---) to the reduced system of equations describing high temperature flows, obtained from a regular perturbation expansion, including terms up to λ^2 , with numerical solutions of the full nonlinear system of equations (—). The material parameters are $e = e_w = 0.8$, $r = 0.6$ and the chute slope is $\tan \theta = 0.3$. Solutions are obtained for a far-field temperature $T_\infty = 50$. For these parameter values the expansion parameter $\lambda \approx 0.27$.

governing equations to the boundary point $s = 1$. However, for an arbitrary c the boundary condition at $s = 1$ will not be satisfied, so c must be iteratively adjusted until this condition is enforced. The value obtained for c depends on the parameter λ . An example of a solution to the high temperature system of equations is shown in figure 13, where the material parameters are $e = e_w = 0.8$, $r = 0.6$ and we have taken a chute slope $\tan \theta \approx 0.354$, which gives $\lambda = 1$. The iterative solution procedure results in a parameter $c = 4.5861$. By comparing with a solution of the full system of equations, we see that the asymptotic solution reproduces the features of the full solution. In particular, the solution exhibits a density inversion even at this high temperature, and this is well approximated by the solution of the asymptotic system.

4.3. Flow domains for high temperature flows

The asymptotic system provides useful approximations to flows at high temperature and, since the system contains a single parameter λ , it is possible to determine the existence of high temperature solutions much more easily than is possible for the full system.

We consider first the case $\delta > 0$, so the high temperature flow is dissipative throughout. In order to balance this energy loss in the flow, the base boundary must be a source of granular temperature and so we require $F_{21} > 0$, and thus $\lambda > 0$. By repeated solution of the asymptotic system of equations we find no solution is possible for $\lambda > 2.284$. We note that for values of λ in the neighbourhood of this upper bound, the numerical solution of the asymptotic system is difficult, since the depth of the flow increases dramatically and the point at which the initial condition should be implemented approaches the singular point at $s = 0$. The accumulation of numerical error may then cause uncertainty in the bound. However, we tentatively use this bound to confine high temperature solutions to the range $0 < \lambda < 2.284$. For fixed material parameters e , e_w and r , these bounds on λ correspond to a finite range

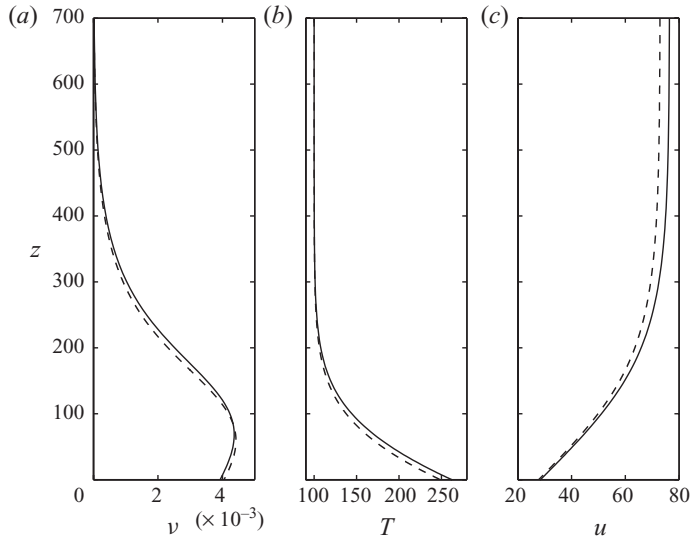


FIGURE 13. Comparison of an approximate solution (---) to the reduced system of equations describing high temperature flows, obtained by solving numerically the simplified system of equations, with a numerical solution of the full nonlinear system of equations (—). The material parameters are $e = e_w = 0.8$, $r = 0.6$ and the chute slope is $\tan \theta \approx 0.354$ which gives $\lambda = 1$. Solutions are obtained for a far-field temperature $T_\infty = 100$.

of chute slopes for which steady solutions can be obtained. In particular the bound $\lambda = 0$ predicts the minimum chute slope for steady flows.

In addition, it is possible to determine the regions where monotonic and inverted density profiles are found. For $\lambda < 0.660$ the volume fraction is monotonic, with the maximum density occurring at the base boundary. In contrast, if $\lambda > 0.660$ the high temperature flows exhibit density inversions. For $e = e_w = 0.8$ and $r = 0.6$, the curve at $\lambda = 0.660$ corresponds to a slope of $\tan \theta = 0.335$ ($\theta = 18.6^\circ$), which is close to the slope of $\tan \theta = 0.33$ at which the qualitative change in behaviour of the macroscopic flow curve is found (as demonstrated in figure 4*b*). We therefore suggest that the change in behaviour of the macroscopic flow curve is a result of density inversion for high temperature flows, and the mid-temperature branch is a signature of the adjustment from monotonic density profiles at high temperature to inverted profiles at low temperature. Our numerical solutions of the full system of equations support this, as seen in figure 4 where the transition from macroscopic Q - h curves with three solutions for a given flow depth coincides with the transition to steady flows which always display a density inversion.

In figure 14(*a*) we show the bounding curves corresponding to $\lambda = 0$ and $\lambda = 2.284$, between which solutions of the high temperature asymptotic system can be obtained. The curves are plotted on the $\tan \theta$ - r plane (for $1/2 < r < \sqrt{3}/2$), and we have taken $e = e_w = 0.8$. We also mark points at which solutions to the full system of equations are found. The high temperature asymptotic system provides good approximations to the boundaries demarking the existence of solutions, as determined by the full system of equations. In particular, the curve corresponding to $\lambda = 0$ is in good agreement with the boundary at which solutions of the full system of equations are found, except for a small region with $\tan \theta > 0.35$, $r > 0.83$ where solutions of the full system of equations exist but high temperature asymptotic solutions are not possible (these solutions of

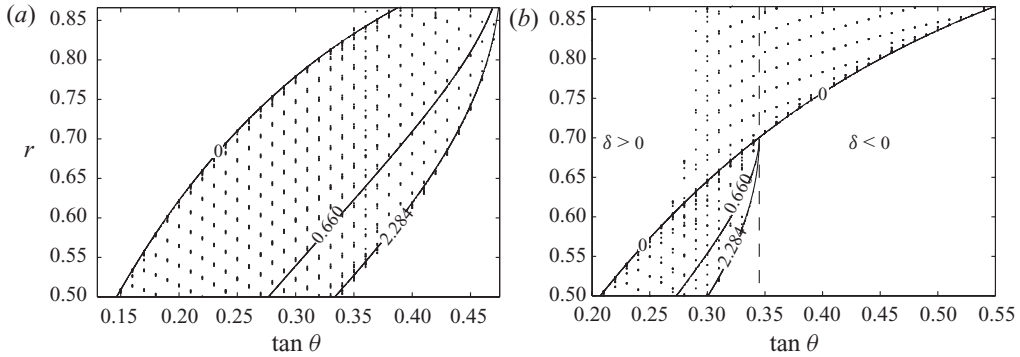


FIGURE 14. The domains of parameter values for which fully developed solutions exist and the predictions of the boundaries from the high temperature asymptotic solutions. In (a) we take coefficients of restitution $e = e_w = 0.8$ resulting in dissipative flow ($\delta > 0$). In (b) the coefficients of restitution are $e = 0.9$ and $e_w = 0.6$ and we find relatively steep slopes result in productive flows ($\delta < 0$) while relatively gentle slopes give dissipative flows. Solutions of the high temperature asymptotic system can be found between the curves corresponding to $\lambda = 0$ and $\lambda = 2.284$, as indicated on the plot. In addition, the curve corresponding to $\lambda = 0.660$ denotes the boundary between monotonic ($\lambda < 0.660$) and inverted ($\lambda > 0.660$) volume fraction profiles. The points mark solutions to the full system of equations with $T_\infty = 1$, $T_\infty = 10$, $T_\infty = 100$ and $T_\infty = 500$.

the full system of equations are of low granular temperature, with $T_\infty = 1$). The cause of this boundary of existence is clear; for $\lambda < 0$ and $\delta > 0$ the boundary is dissipative and so too is the flow, so there is no possible energy balance. On the other hand, the boundary at $\lambda = 2.284$ provides a less accurate approximation of the existence boundary, perhaps due to the numerical errors in the solution of the asymptotic system. Since the direction of the boundary flux here is consistent with the dissipation within the flow, the existence boundary here results from an inability to match the magnitude of the energy fluxes, so the dissipation in the flow is insufficient to remove the energy supplied by the base boundary.

Let us now consider the case $\delta < 0$, corresponding to high temperature flows which are productive in the interior. It is clear that we now require a flux of granular temperature into the base boundary in order to remove the fluctuation energy from the flow, so require $F_{21} < 0$ and thus $\lambda < 0$. On repeatedly solving the high temperature asymptotic system, varying the parameter λ , we are unable to find a lower bound on λ , suggesting high temperature solutions are possible whenever $\delta < 0$ and $\lambda < 0$. Furthermore all high temperature flows we find have monotonic volume fraction profiles. On taking the coefficients of restitution $e = e_w = 0.8$, it is not possible to choose $r \in [1/2, \sqrt{3}/2]$ and $\tan \theta$ such that $\delta < 0$ and $\lambda < 0$, so no high temperature productive flows are possible. If instead we take $e = 0.9$ and $e_w = 0.6$, so that there is less dissipation in the flow but more at the base boundary, then it is possible to obtain flows with productive interiors and a dissipative base boundary. The bounding curves of the high temperature asymptotic system and some solutions of the full system are shown in figure 14(b). For these parameter values it is possible to find solutions to the full system of equations in a region with $\delta > 0$ and $\lambda < 0$, where no solutions of the high temperature asymptotic system are possible. Solutions in this region cannot be classified as productive or dissipative, but rather are productive in some parts of the interior of the flow and dissipative in others. Such behaviour cannot be described by the high temperature asymptotic analysis. Furthermore, solutions of the

full system of equations in this region cannot be found for arbitrarily large far-field granular temperature. However, for those parameter values which result in either purely productive or purely dissipative flows, the boundaries obtained from the high temperature asymptotic analysis can be used to predict the domains in parameter space where steady solutions can be found.

The boundary curves, given in terms of the parameter λ , can be recast to give the range of inclination angles for which steady flows are possible. For dissipative flows, for which $\delta > 0$, we find solutions of the high temperature system for $0 < \lambda < \lambda_c$, where $\lambda_c = 2.284$. Recasting these bounds in terms of the chute slope, we find dissipative flows for inclination angles with $\tan^2 \theta < L/M$, where

$$L = \frac{\pi \lambda_c g_{30} g_{52}}{3}, \quad M = \frac{\pi \lambda_c g_{30}}{3 g_{20}}. \quad (4.25)$$

This condition follows from the inequality $\delta > 0$ (note $L/M = g_{20} g_{52}$). Further we have shown that solutions with high granular temperatures require $0 < \lambda < \lambda_c$ and this implies the more restrictive condition that $l/m < \tan^2 \theta < \tan^2 \theta_0$, where it is convenient to define

$$l = \frac{2(1 - e_w)}{1 + \sqrt{1 - r^2}}, \quad m = \frac{\pi}{2\kappa} - \sqrt{\frac{\pi}{2} \frac{A_0 r^2}{2\kappa g_{20}}}, \quad (4.26)$$

and $\tan \theta_0$ is defined by

$$m \tan^2 \theta_0 - l = (L - M \tan^2 \theta_0)^{1/2}. \quad (4.27)$$

The functions l , m , L and M determine the energy balance of the flow, with l and m representing the loss of energy at the base due to inelastic collisions, and the production of energy at the base due to shear work, respectively. Furthermore L can be associated with the dissipation of energy within the flow interior due to inelastic collisions, and M represents the production of energy in the interior of the flow by shear work. For productive flows, for which $\delta < 0$, high temperature solutions are possible for $\lambda < 0$. We therefore find productive flows for inclination angles with $\tan^2 \theta > L/M$, and high temperature solutions can be found for $L/M < \tan^2 \theta < l/m$. These bounds on the chute slope are qualitatively similar to those obtained by Anderson & Jackson (1992) from an analysis of flows at high density, and the functions l , m , L and M can be compared to the functions obtained in this earlier study.

5. Conclusion

A continuum description of rapid granular flows, derived from a granular kinetic theory, has been used to model grain flows down an inclined planar chute. We have developed a mapped Chebyshev pseudospectral method to obtain highly accurate numerical approximations to solutions corresponding to steady fully developed flows.

The kinetic theory continuum model introduces several parameters which control the character of the steady solutions. By coupling the pseudospectral solution scheme to a parametric continuation algorithm we are able to investigate efficiently the influence of the controlling parameters on the steady solutions. We obtain solutions in which the interior of the flow is dissipative, and here the density profiles can be inverted or monotonically decreasing, and flows which are productive in the interior

and the density decreases monotonically. The character of the solutions is robust to a change from asymptotic surface conditions to interface conditions.

We characterize solutions using depth-integrated variables, in particular the mass flux of material and the centre-of-mass, and determine the relationship between these macroscopic variables. We find regions of parameter space where multiple solutions are obtained for a specified mass flux of material. In some regions of parameter space, three flows of differing depth are found for a fixed mass flux, in other regions there is a minimum mass flux for steady solutions and above this minimum two distinct flows are found for a specified mass flux. The transition to families of solutions with two flows of equal mass flux coincides with a change in behaviour of the solution profiles at high temperature, from flows with monotonic density profiles to density inverted flows. In some other regions of parameter space, where the flows are productive in the interior and the base is dissipative, we find a single solution for a specified mass flux.

Steady solutions are found only in certain domains in the parameter space. It is difficult to determine these domains *a priori*, but through an asymptotic analysis of the governing equations, appropriate to dilute, high temperature flows, we are able to obtain a simplified, although still nonlinear, system of equations from which we are able to predict the domains of existence. In addition, the asymptotic system predicts a transition in the high temperature solutions from monotonic to inverted density profiles. The point at which this transition occurs is in close correspondence with a transition seen in the macroscopic flow curves, where there is a change from curves displaying three solutions for a specified mass flux to curves where we always obtain two distinct solutions. This correspondence leads us to suggest that the transition from monotonic to density inverted flows at high temperature results in the transition between the Q - h relationship on gentle slopes, where there is a finite region where three steady solutions with equal mass flux can be found and outside of this region only one steady solution is obtained, and the relationship on steep slopes, where there is a minimum mass flux for which steady solutions exist and above this minimum value we can always obtain two solutions for a given mass flux. Our numerical solutions of the full system of equations support this view. We have also shown through our asymptotic analysis that for highly agitated, dilute flows we have a scaling relationship $h \sim Q^2$, which is markedly different from the Bagnold relationship $h \sim Q^{2/5}$ which is obtained when the volume fraction is constant.

Although we have obtained steady flow solutions from the kinetic theory continuum model, we may be unable to observe these solutions in experimental realizations. If a steady flow is unstable to small perturbations then it is unlikely to be observed in an experiment. In part 2 of this paper we assess the linear stability of the steady solutions to small perturbations in both the downslope and cross-slope directions, extending the methodology of Forterre & Pouliquen (2002) and Mitarai & Nakanishi (2004). We also note that the kinetic theory of Lun & Savage (1986) neglects frictional interactions and enduring contacts in the microscopic interactions, and therefore this simple kinetic theory continuum description may be unable to reproduce fully experimental observations. As the granular kinetic theory continues to develop, for example, by accounting for frictional interactions (Jenkins & Zhang 2002) and the development of enduring contacts (Jenkins 2007; Kumaran 2008), we anticipate a closer correspondence between predictions and observations. The methodology we have developed could be utilized to obtain solutions from these extended continuum models.

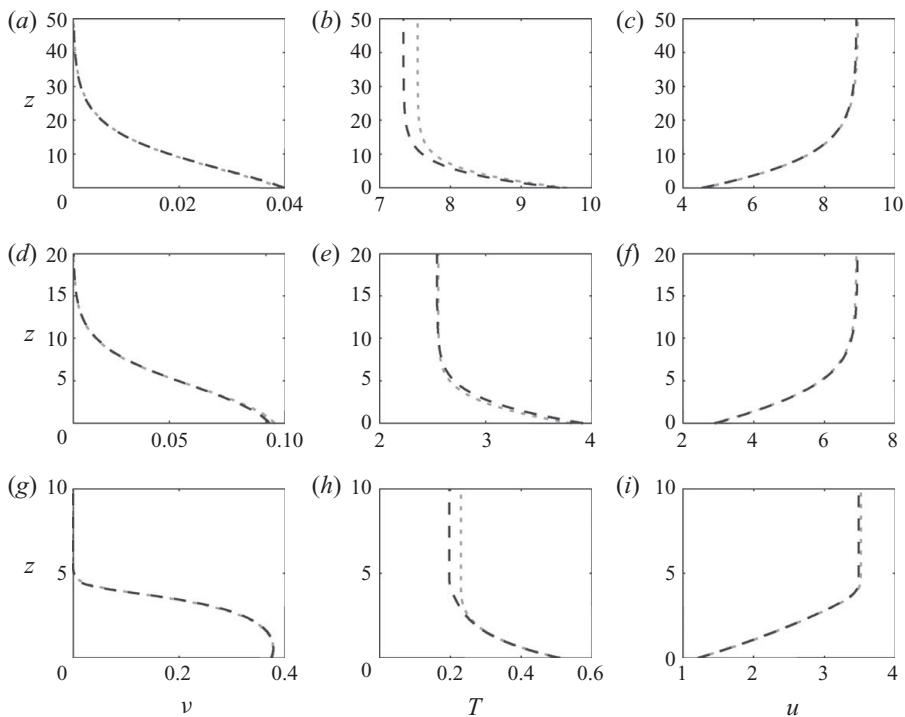


FIGURE 15. A comparison of the solution profiles obtained with the reduced heat flux (. . .) (taking $g_4 \equiv 0$) with the corresponding solutions with the modified Fourier heat flux (---). For a specified mass flux of $Q = 3$ three solutions are found; (a–c) high temperature flow; (d–f) mid-temperature flow; (g–i) low temperature flow. The material parameters are $e = e_w = 0.8$, $r = 0.6$ and the chute slope is $\tan \theta = 0.3$.

M.J.W. and A.A.S. are grateful to the EPSRC for funding through doctoral training grants. We thank Richard Kerswell and James Jenkins for informative discussions.

Appendix. Steady solutions with a Fourier heat flux

The granular kinetic theory of Lun *et al.* (1984) results in a modified Fourier form of the heat flux, with a term proportional to $\nabla \nu$. The modified Fourier heat flux also appears in a similar form in the constitutive theories of Sela & Goldhirsch (1998) and Garzó & Dufty (1999). This feature has been shown to be an important characteristic of vibro-fluidized granular beds (Soto, Mareschal & Risso 1999; Brey *et al.* 2001; Ramírez & Soto 2003; Huan *et al.* 2004). Previous chute flow studies (Forterre & Pouliquen 2002; Mitarai & Nakanishi 2004) discarded the conduction along density gradients. Here we show that retaining this term does not qualitatively change the character of the solutions we obtain. The solutions with the Fourier form of the heat flux are found by setting the constitutive function $g_4 \equiv 0$.

In figure 15 we show flow solutions for a specified mass flux $Q = 3$, comparing the profiles obtained with the reduced heat flux with the corresponding solution with the modified Fourier heat flux (which are shown in figure 2). The character of the solutions is not affected by the form of the heat flux term, with the difference between the solutions most apparent in the granular temperature profiles.

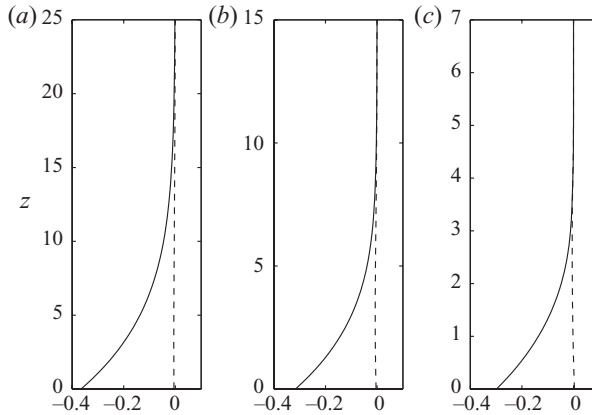


FIGURE 16. Comparison of terms contributing to the heat flux for (a) the high temperature steady flow, (b) the mid-temperature steady flow and (c) the low temperature steady flow with mass flux $Q = 3$. The heat flux along temperature gradients (—, $g_3 T^{1/2} (dT/dz)$) dominates the flux along volume fraction gradients (---, $g_4 T^{3/2} (dv/dz)$) for each of the flows. The material parameters are $e = e_w = 0.8$, $r = 0.6$ and the chute slope is $\tan \theta = 0.3$.

The small influence of this term representing a heat flux along density gradients can be seen in figure 16, where the two terms contributing to the heat flux are shown for the three steady solutions with mass flux $Q = 3$. The heat flux along temperature gradients dominates the flux along volume fraction gradients, and therefore the solutions with a Fourier form for the heat flux differ little from those where the modified Fourier form is retained.

Although the modification of the Fourier heat flux to include a contribution along density gradients introduces only a subdominant term into the heat flux for the steady flows in figure 15, there is an observable effect on the granular temperature profile. This can be understood through an asymptotic analysis of the governing equations in regions where the volume fraction and heat flux are small, as in §3.2. With the modified Fourier form the temperature field behaves as

$$T = T_\infty + \frac{g_{40}}{g_{30}} T_\infty a e^{-z/T_\infty} \quad \text{for } z \gg 1, \tag{A 1}$$

from (3.24), where a is an undetermined constant. In contrast, if the heat flux along volume fraction gradients is neglected, so $g_4 \equiv 0$, we find,

$$T = T_\infty - \frac{a^2}{4g_{30}} \left(\frac{\tan^2 \theta}{g_{20}} - g_{52} \right) T_\infty^3 e^{-2z/T_\infty} \quad \text{for } z \gg 1, \tag{A 2}$$

so the temperature field decays more rapidly to the far-field value if $g_4 \equiv 0$. This behaviour is seen in figure 15, particularly for the low temperature flow.

Finally, the form of the heat flux also has only a small influence on macroscopic flow variables used to describe the flow, with the character of the $Q-h$ curve unaffected by taking $g_4 \equiv 0$, as shown in figure 17.

We conclude that the character of the steady solutions, for the parameter values studied, is unaffected by the form of the heat flux. However, if the grains are made less elastic, by reducing the coefficient of restitution, the modification to the Fourier form

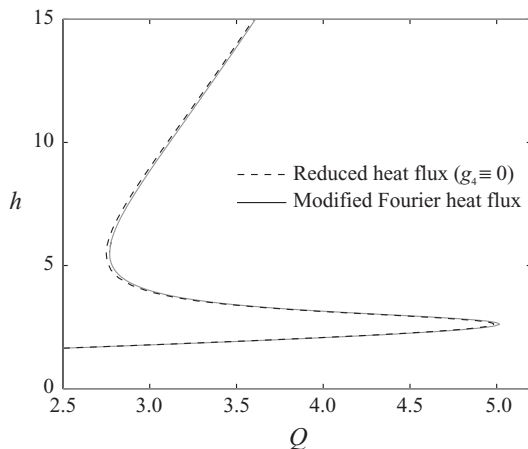


FIGURE 17. The centre-of-mass h as a function of mass flux Q obtained with the reduced heat flux (taking $g_4 \equiv 0$), with the corresponding curve with the modified Fourier heat flux, as indicated. The material parameters are $e = e_w = 0.8$, $r = 0.6$ and the chute slope is $\tan \theta = 0.3$.

becomes more important, since the constitutive function $g_4 \sim (1 - e)$. Furthermore, in geometries other than the chute flow, or when sidewalls are imposed, the concentration gradients may be stronger than those observed here and then the influence of the modified heat flux will be stronger.

REFERENCES

- ABRAMOWITZ, M. & STEGUN, I. A. (Ed.) 1965 *Handbook of Mathematical Functions*, 9th edn. Dover.
- AHN, H., BRENNEN, C. E. & SABERSKY, R. H. 1991 Measurements of velocity, velocity fluctuation, density, and stresses in chute flows of granular materials. *J. Appl. Mech.* **58**, 792–803.
- AHN, H., BRENNEN, C. E. & SABERSKY, R. H. 1992 Analysis of the fully developed chute flow of granular materials. *J. Appl. Mech.* **59**, 109–119.
- ANDERSON, K. G. & JACKSON, R. 1992 A comparison of the solutions of some proposed equations of motion of granular materials for fully developed flow down inclined planes. *J. Fluid Mech.* **241**, 145–168.
- AZANZA, E., CHEVOIR, F. & MOUCHERONT, P. 1999 Experimental study of collisional granular flows down an inclined plane. *J. Fluid Mech.* **400**, 199–227.
- BOYD, J. P. 2000 *Chebyshev and Fourier Spectral Methods*, 2nd edn. Dover.
- BREY, J. J., RUIZ-MONTERO, M. J. & MORENO, F. 2001 Hydrodynamics of an open vibrated granular system. *Phys. Rev. E* **63**, 061305/1–10.
- CAMPBELL, C. S. 1990 Rapid granular flows. *Annu. Rev. Fluid Mech.* **22**, 57–92.
- CAMPBELL, C. S. & BRENNEN, C. E. 1985 Chute flows of granular material: some computer simulations. *J. Appl. Mech.* **52**, 172–178.
- CHAPMAN, S. & COWLING, T. G. 1970 *The Mathematical Theory Of Non-Uniform Gases*, 3rd edn. Cambridge University Press.
- DRAKE, T. G. 1991 Granular flow: physical experiments and their implications for microstructural theories. *J. Fluid Mech.* **225**, 121–152.
- FORTERRE, Y. & POULIQUEN, O. 2001 Longitudinal vortices in granular flows. *Phys. Rev. Lett.* **86** (26), 5886–5889.
- FORTERRE, Y. & POULIQUEN, O. 2002 Stability analysis of rapid granular chute flows: formation of longitudinal vortices. *J. Fluid Mech.* **467**, 361–387.
- FORTERRE, Y. & POULIQUEN, O. 2008 Flows of dense granular media. *Annu. Rev. Fluid Mech.* **40**, 1–24.
- GARZÓ, V. & DUFTY, J. W. 1999 Dense fluid transport for inelastic hard spheres. *Phys. Rev. E* **59** (5), 5895–5911.

- GOLDHIRSCH, I. 2003 Rapid granular flows. *Annu. Rev. Fluid Mech.* **35**, 267–293.
- HAFF, P. K. 1983 Grain flow as a fluid-mechanical phenomenon. *J. Fluid Mech.* **134**, 401–430.
- HANES, D. M. & WALTON, O. R. 2000 Simulations and physical measurements of glass spheres flowing down a bumpy incline. *Powder Technol.* **109**, 133–144.
- HUAN, C., YANG, X., CANDELA, D., MAIR, R. W. & WALSWORTH, R. L. 2004 NMR experiments on a three-dimensional vibrofluidized granular medium. *Phys. Rev. E* **69**, 041302/1–13.
- JAEGER, H. M., NAGEL, S. R. & BEHRINGER, R. P. 1996 Granular solids, liquids, and gases. *Rev. Mod. Phys.* **68** (4), 1259–1273.
- JENKINS, J. T. 2006 Dense shearing flows of inelastic disks. *Phys. Fluids* **18**, 103307/1–9.
- JENKINS, J. T. 2007 Dense inclined flows of inelastic spheres. *Granul. Matter* **10**, 47–52.
- JENKINS, J. T. & HANES, D. M. 1993 The balance of momentum and energy at an interface between colliding and freely flying grains in a rapid granular flow. *Phys. Fluids A* **5** (3), 781–783.
- JENKINS, J. T. & RICHMAN, M. W. 1985 Grad's 13-moment system for a dense gas of inelastic spheres. *Arch. Rat. Mech. Anal.* **87** (4), 355–377.
- JENKINS, J. T. & SAVAGE, S. B. 1983 A theory for the rapid flow of identical, smooth, nearly elastic, spherical particles. *J. Fluid Mech.* **130**, 187–202.
- JENKINS, J. T. & ZHANG, C. 2002 Kinetic theory for identical, frictional, nearly elastic spheres. *Phys. Fluids* **14**, 1228–1235.
- JOHNSON, P. C. & JACKSON, R. 1987 Frictional–collisional constitutive relations for granular materials, with application to plane shearing. *J. Fluid Mech.* **176**, 67–93.
- JOHNSON, P. C., NOTT, P. & JACKSON, R. 1990 Frictional–collisional equations of motion for particulate flows and their applications to chutes. *J. Fluid Mech.* **210**, 501–535.
- KUMARAN, V. 1998a Kinetic theory for a vibro-fluidized bed. *J. Fluid Mech.* **364**, 163–185.
- KUMARAN, V. 1998b Temperature of a granular material “fluidized” by external vibrations. *Phys. Rev. E* **57** (5), 5660–5664.
- KUMARAN, V. 2008 Dense granular flow down an inclined plane: from kinetic theory to granular dynamics. *J. Fluid Mech.* **599**, 121–168.
- LUN, C. K. K. & SAVAGE, S. B. 1986 The effects of an impact velocity dependent coefficient of restitution on stresses developed by sheared granular materials. *Acta Mech.* **63**, 15–44.
- LUN, C. K. K., SAVAGE, S. B., JEFFREY, D. J. & CHEPURNIY, N. 1984 Kinetic theories for granular flow: inelastic particles in Couette flow and slightly inelastic particles in a general flowfield. *J. Fluid Mech.* **140**, 223–256.
- MCMANARA, S. & YOUNG, W. R. 1992 Inelastic collapse and clumping in a one-dimensional granular medium. *Phys. Fluids A* **4** (3), 496–504.
- MCMANARA, S. & YOUNG, W. R. 1994 Inelastic collapse in two dimensions. *Phys. Rev. E* **50** (1), 28–31.
- MITARAI, N. & NAKANISHI, H. 2004 Linear stability analysis of rapid granular flow down a slope and density wave formation. *J. Fluid Mech.* **507**, 309–334.
- MITARAI, N. & NAKANISHI, H. 2005 Bagnold scaling, density plateau, and kinetic theory analysis of dense granular flow. *Phys. Rev. Lett.* **94**, 128001/1–4.
- NOTT, P. & JACKSON, R. 1992 Frictional–collisional equations of motion for granular materials and their application to flow in aerated chutes. *J. Fluid Mech.* **241**, 125–144.
- RAMÍREZ, R. & SOTO, R. 2003 Temperature inversion in granular fluids under gravity. *Physica A* **322**, 73–80.
- RHEINBOLDT, W. C. 1986 *Numerical Analysis of Parametrized Nonlinear Equations*, University of Arkansas Lecture Notes in the Mathematical Sciences, vol. 7. John Wiley & Sons.
- RICHMAN, M. W. 1988 Boundary conditions based upon a modified Maxwellian velocity distribution for flows of identical, smooth, nearly elastic spheres. *Acta Mech.* **75**, 227–240.
- RICHMAN, M. W. & MARCINIEC, R. P. 1990 Gravity-driven granular flows of smooth, inelastic spheres down bumpy inclines. *J. Appl. Mech.* **57**, 1036–1043.
- SAVAGE, S. B. 1979 Gravity flow of cohesionless granular materials in chutes and channels. *J. Fluid Mech.* **92**, 53–96.
- SELA, N. & GOLDHIRSCH, I. 1998 Hydrodynamic equations for rapid flows of smooth inelastic spheres, to Burnett order. *J. Fluid Mech.* **361**, 41–74.
- SELLAR, A. A. 2003 Free-surface rapid granular flows. PhD thesis, School of Mathematics, University of Bristol.

- SILBERT, L. E., ERTAŞ, D., GREST, G. S., HALSEY, T. C., LEVINE, D. & PLIMPTON, S. J. 2001 Granular flow down an inclined plane: Bagnold scaling and rheology. *Phys. Rev. E* **64**, 051302/1–14.
- SILBERT, L. E., GREST, G. S., BREWSTER, R. & LEVINE, A. J. 2007 Rheology and contact lifetimes in dense granular flows. *Phys. Rev. Lett.* **99**, 068002/1–4.
- SILBERT, L. E., GREST, G. S., PLIMPTON, S. J. & LEVINE, D. 2002 Boundary effects and self-organization in dense granular flows. *Phys. Fluids* **14** (8), 2637–2646.
- SOTO, R., MARESCHAL, M. & RISSO, D. 1999 Departure from Fourier’s law for fluidized granular media. *Phys. Rev. Lett.* **83** (24), 5003–5006.
- WALTON, O. R. 1993 Numerical simulation of inclined chute flows of monodisperse, inelastic, frictional spheres. *Mech. Mater.* **16**, 239–247.
- WOODHOUSE, M. J. & HOGG, A. J. 2010 Rapid granular flows down inclined planar chutes. Part 2. Linear stability analysis of steady flow solutions. *J. Fluid Mech.* Forthcoming.
- ZHENG, X. M. & HILL, J. M. 1996 Molecular dynamics modelling of granular chute flow: density and velocity profiles. *Powder Technol.* **86**, 219–227.